HANFORD IFRC QUARTERLY REPORT ~ JULY 2009

John M. Zachara and the IFRC Team
Pacific Northwest National Laboratory

I. Overview and Highlights

This is the fourth Quarterly Report for the Hanford IFRC project that summarizes significant progress for the period of January 2009 to July 2009. Six major highlights deserve mention for this reporting period that will be discussed in sections that follow.

1. Our first phase of laboratory characterization measurements of physical and geochemical properties on 109 grab samples from IFRC boreholes has been completed.
2. A second large scale, non-reactive tracer experiment was successfully performed in March 2009 during a period of low and stable Columbia River stage. The experiment involved the injection of chilled (to 8 °C), Br^- and D_2O-spiked groundwater with plume monitoring by the in-situ thermistor array, downhole Br ion selective electrodes, and laboratory analyses of Br and D_2O. The experiment design was assisted by premodeling using updated hydrogeological parameters for the site determined by the first tracer experiment.
3. Our first phase of geophysical characterization of the IFRC well field was completed using the down-hole ERT array and a newly purchased data logger. The geophysical measurements were processed by inversion modeling to yield a 3-D model of electrical properties throughout the IFRC experimental domain. Laboratory measurements have been initiated to link electrical response with sediment and grain distribution properties relevant to transport.
4. A spring passive experiment was completed at the IFRC site. The experiment monitored U(VI) mobilization from the smear zone, and overall compositional changes to groundwater at multiple depths as high Columbia River stage waters resulting from snow-melt caused an extended and significant water table rise and fall event. Over 1000 samples were collected for chemical analyses that were synchronized with continuous monitoring of river stage; and groundwater elevations, temperature, and specific conductivity.
5. A series of three laboratory-scale U(VI) reactive transport experiments with intact IFRC cores from the upper, middle, and lower thirds of the saturated zone are nearing completion in collaboration with PNNL's Subsurface Focus Area (SFA). The experiments provide insights and quantification of in-situ reactive transport parameters for U. The experiments were of complicated design, and results have been modeled with one of several approaches to be tried.
6. The modeling team is integrating new hydrologic and thermal data from characterization measurements and the first tracer experiment, and geochemical data from laboratory characterization measurements and the intact column experiments into an improved transport model of the IFRC site for use in interpretation of the spring passive transport experiment and subsequent injection experiments with U.

II. Significant Changes

There have been no significant changes to the project scope or objectives since the last quarterly report in January 2009.

III. Management & Operations

Management and operations of the Hanford IFRC have proceeded without major problems over the two past reporting quarters. Site completion, characterization, lab/field experimentation, model and project spending has proceeded as planned, and the project overall is on schedule with milestones.

IV. Quarterly Highlights

Task 1. Project Management

IFRC project management is proceeding as smoothly as can be expected, and there are no outstanding issues with finances, staffing, subcontracts, project productivity, site infrastructure or access, schedule, or modeling. The Hanford IFRC project team held a project meeting, and presented a series of posters and a dedicated plenary session at the ERSD P.I. meeting in April, 2009. The team received many positive comments on the quality and innovative aspects of our field experimental site, progress of laboratory characterization measurements and field experiments, and significance of scientific findings.

To great extent the project is moving forward according to the PI's expectations, but feedback from ERSD and the FREC is solicited. At this point the project team is working actively to complete manuscripts on: the first two injection experiments, results of field and laboratory characterization measurements, and the development of improved site hydrogeologic and geochemical models. Active planning is also underway for field experiments to be performed in the summer (FY09) and fall (FY10) of 2009.

In the process of updating the discharge permit for the Spring experiment, the project determined that the Washington State Waste Discharge Permit ST 4511 that covers injections at the IFRC site allows up to 27 injection wells to be used, rather being tied to specific locations. This gives the project maximum flexibility for selecting different injection points to meet our scientific objectives. Thus far, the same injection well was used for both field experiments, but future experiments may use other injection well locations.

Task 2. Site Design and Installation

The Borehole Drilling, Sampling, and Well Construction Report was completed and posted on the Hanford IFRC web-site in early February 2009. The report provides a comprehensive description of the installed IFRC well-field, well completion details, and

a conceptual hydrogeologic model for the site. This report concludes activities in this task for FY09.

Task 3. Website and Data Management

There were no new or significant modifications to the IFRC data base. However, the posting of completed data sets has been given priority. Additionally, the data management effort is focusing on integrating the experimental data in a coherent framework, and adding a forum capability and an interactive animation capability for time-series data (temperature data, water-level data and the like) to the IFRC database. In conjunction with this new capability, an internal report will be prepared documenting all the IFRC related data as well as the underlying data models and access capabilities. This is expected to result in a publication in September 2009 tentatively titled "An integrated web accessible data set for the 300 Area IFRC", aimed at Computer and Geosciences.

Task 4. Field Site Characterization

The IFRC well field, and samples obtained during the drilling campaign, are being characterized according to the Hydrologic and Geochemical Characterization Plan that is posted on the web. Significant progress has been made.

Geophysical Characterization

Instrumentation: A new multi-channel DAS-1 Electrical Impedance Tomography system (Multi-phase Technologies LLC) was delivered in late March 2009 and put into service. This purchase was made possible with ERSD capital funds that are appreciated. The DAS-1 is a fully autonomous, 8-channel system capable of collecting 3-D subsurface images using Electrical Resistivity Tomography (ERT) or Electrical Impedance Tomography (EIT) using 240 electrodes simultaneously. It is now possible with this system to interrogate eight wells at a time, or the whole electrode array with well sub-sampling. Furthermore, there has been an 8-fold increase in acquisition speed which should allow monitoring of flow and transport processes. This system has three data acquisition modes: i.) time domain, ii.) frequency domain, and iii.) data stream mode. The time domain mode collects IP data using 1 to 35 user assignable windows at base frequencies from 1/64 Hz to 9 Hz. The frequency domain mode acquires amplitude and phase data over the range 1/64 Hz to 5 Hz. The data stream mode stores signal from up to 128 points for later analysis with user-supplied averaging and noise rejection techniques. This system is now fully functional although field tests have indicated that firmware upgrades are needed to take advantage of all the capabilities.

3-D Distribution of Electrofacies: Interpreting the stratigraphy, lithology, and hydrogeology of subsurface units has historically depended on core samples and borehole logs. Considerable information on the IFRC site has been derived from studies of samples collected during installation of the well field. While the sedimentary facies defined from cores provide good vertical geological information, it is of limited lateral extent. In order to extrapolate this information to the complete well dataset, borehole logs are being

calibrated on cored intervals, and a classification system developed based on gamma-ray and neutron thermalization measurements and electrofacies distribution.

Over the last quarter, efforts associated with the recognition, classification and prediction of electrofacies using surface electrical resistivity, crosshole resistivity tomograms, and well logs continued with the goal of building electrofacies-specific hydraulic property correlations. Electrical resistivity surveys were initiated with a single-channel MPT system using four wells at a time with a two-well overlap. Receipt of the new multi-channel DAS-1 Electrical Impedance Tomography system allowed complete characterization of the 3-D distribution of electrical properties in early April. These data are being analyzed at INL. A model consisting of some 640,046 elements and 149,706 data points collected from 840 electrodes was inverted to develop the 3-D distribution of electrical properties. This was accomplished using 360 processors requiring about 6 hours of run time. The 3-D inversion of the 2-D resistivity lines involved 1833 electrodes, 132300 data points and 512,509 model elements. Inversion was accomplished with 460 processors and required about 8 hours of run time. The result is our first iteration of a 3-D field-scale model for the distribution of electrofacies for the 300 Area (Figure 1), with a more detailed distribution for the IFRC site (Figure 2).

Analyses thus far show three major facies types with distinct electrical resistivities and chargeability characteristics are present within the IFRC site. All of the surveys show a low resistivity high chargeability anomaly west of the old south process pond (SPP; orange in Figure 1).

This anomaly could be due to a variety of accumulated materials (e.g., dissolved metal cladding of rejected fuel assemblies, fly ash, strong electrolytes or other processing wastes). Chargeability is known to depend on a number of factors, including mineral type, grain size, the ratio of internal surface area to volume, the properties of electrolytes

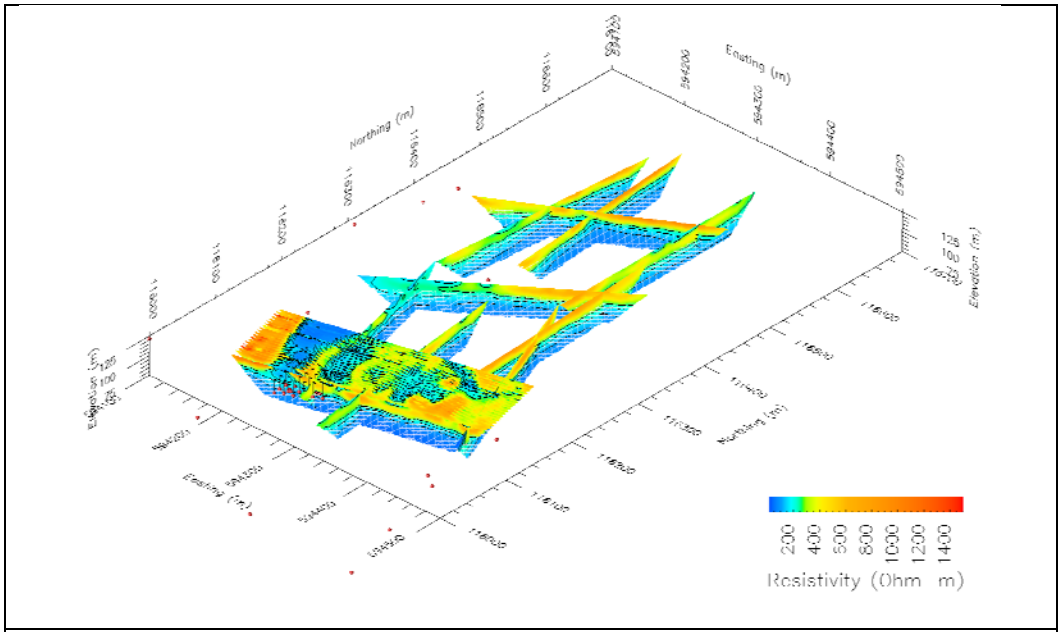

Figure 1. Three-dimensional distribution of electrofacies in the 300 Area.

in pore space, and sediment-fluid interfacial interaction. The relationship of field measurements to variations in lithology will improve as the contribution of these factors is better understood through laboratory measurements and correlation.

Geophysical measurements have also allowed the estimation of spatial variations in the Hanford-Ringold interface for the 300 Area, in general, and for the IFRC site. Prior to the installation of the IFRC well field, the absence of wells in the SPP prevented robust interpretation of the local lithology. The collection of dense 2-D electrical resistivity data and the completion of the 3D cross well measurements now allow for a much-improved description of variations in lithology above the Hanford-Ringold interface. The mean and standard deviation of resistivity values were computed at known interface depths derived from IFRC wells to estimate the depth to the interface. At present, the 3D inversions are still of relatively low resolution as they utilized a smooth inversion based on standard regularization.

IFRC characterization research is continuing to integrate log-derived information on stratigraphy, lithology, and hydrogeology through electrofacies analysis. At present the ERT inversion code is being modified to allow the use of prior information (e.g., borehole logs) and geostatistical constraints within the inversion code. Geostatistics, i.e.

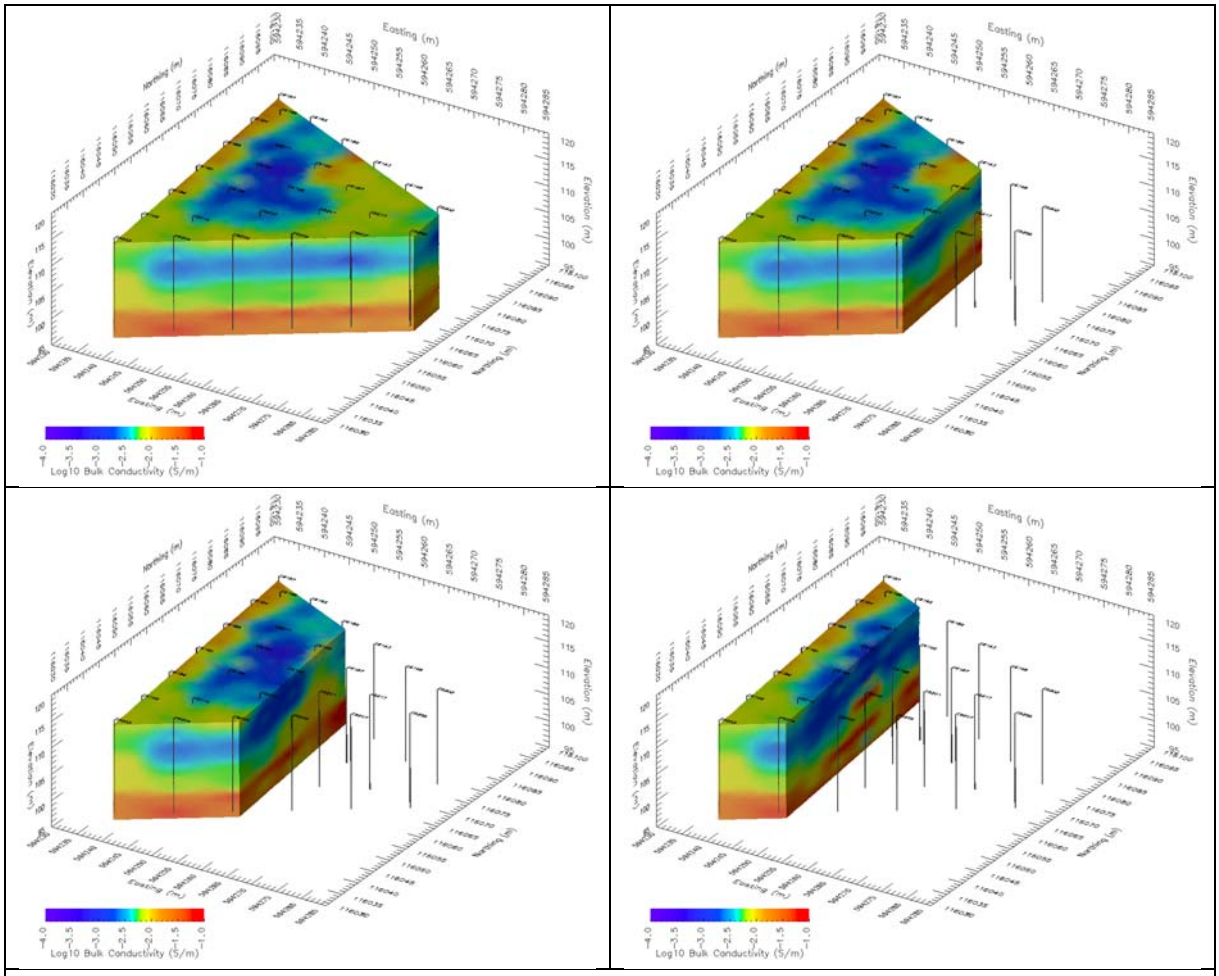

Figure 2. Three-dimensional distribution of electrofacies at the IFRC Site.

the directional and zonal semi-variograms, derived from borehole electromagnetic induction (EMI) logs will be used as a constraint. It is expected that the next iteration of the 3D electrofacies map will include and fit all of the ERT data, obey the geostatistics inferred from the borehole logs (including uncertainty in the semi-variograms), and honor the conductivity values at the wells given by the EMI logs. The suite of solutions should then allow estimation of characterization uncertainty (i.e., mean and variance, etc.). The collection of density and porosity logs during FY10 should allow further improvements to the overall site geophysical/lithologic model.

Characteristics of Preferential Flow Paths: Investigations continued into the application of electrical resistivity measurements to better characterize the subsurface, and to map variations in hydrophysical properties. An azimuthal square-array resistivity survey was conducted over the IFRC well field to assess the ability of surface d.c. resistivity methods to detect preferential flow paths. This type of survey allows measurement of azimuthal variations in apparent resistivity, and is sensitive to subsurface anisotropy. Such variations have been shown to be related to zones of fractures with similar orientations and water-producing fracture zones in crystalline bedrock. They may consequently provide insight into the strike and dip of preferential paths within the complex porous media present within the IFRC site.

The square-array method was field tested at the IFRC field site during the last quarter. At this site, approximately 5 m of clean gravelly sand backfill is underlain by the sand dominated Hanford formation, with the Ringold formation occurring at a mean depth of 16.8 m. The water table is around 9 m depending on season. The survey consisted of seven square soundings separated by a 15° rotational angle about well 399-2-18 (C6196), the array center point. The A-spacings of the arrays were expanded from 5 m to 50 m (in increments of $2^{1/2}$) for each sounding. The electrode locations were optimized to avoid trailers and other obstructions, and installed to centimeter accuracy with a real time kinematic global positioning system. Each electrode was watered using a knapsack sprayer to improve coupling with the sediment. Resistivity data were collected using the new MPT DAS-1 system using the full multiplexing capability. This allowed a complete sounding at a given azimuth to be collected through remotely accessed switches that automatically connected electrodes for a given measurement.

A polar plot of the azimuthal apparent resistivities collected during the first set of surveys is displayed in Figure 3. The effective exploration depths of the survey were 7, 10, 14, 20, 28, and 40 m. These data show significant variation in apparent resistivity for the different azimuthal array orientations for all A-spacings. The almost perfect circle formed by the data from the 7-m A-spacing is indicative of a relatively isotropic layer. This plot delineates the overburden as the top 5 m or so, consisting of "clean" backfill that was used to replace excavated contaminated materials. All other resistivities beyond this depth show a progressive increase in asymmetry, suggesting an increase in anisotropy with depth. However, the degree of anisotropy and the orientation of maximum resistivity are both dependent on depth. At the 10- and 14-m A-spacings, the maximum resistivity measured is parallel to a trend of 75° with a preferential path whose strike of around 165°. At 28- and 40-m, the trend in maximum resistivity is close to 90°

with a strike of only 170° or so. Assuming that the response is due entirely to anisotropy in the formation, the azimuthal apparent resistivities suggest a preferential path with a mean strike of between 150° and 170°. The orientation of the preferential path strike interpreted from square-array data agrees qualitatively with the geologists logs that suggest an incision into the Ringold formation with a southeasterly strike. Such a southeasterly preferential path strike is also evident from the behavior of tracer and temperature plumes in the March injection experiment. Rigorous analysis of these data will also allow estimates of the porosity variations of the different domains.

The azimuthal apparent resistivities can also be affected by spatial (heterogeneity) and temporal variations (transport) in resistivity. For example, strike may be expected to vary with season as the water level changes. Thus, these measurements will be repeated over time to gain better insight in the physical phenomena controlling transport behavior. Surveys with a number of different electrode configurations, are currently being designed to isolate the effects of heterogeneity from anisotropy. These will be implemented in the coming months.

Heat Tracer Experiments: The hydraulic transport of heat enables its use as a tracer. Thus, as an alternative to chemical tracers, variations (passive or active) in groundwater temperature afford the opportunity to use heat to quantify the 3-D water flux. Wiring and automation of the thermistor array (840 sensors) were completed in December 2008 and, since then, water temperature has been monitored on a near continuous basis. The mean groundwater temperature at the IFRC well field is ≈ 17 °C, while the river water temperature can range from ≈ 5 - 17 °C.

The first temperature experiment was conducted in March 2009 and was intended to evaluate the ability of the thermistor array to track temperature anomalies and provide a dataset that could be used to optimize the design of subsequent experiments. Chilled groundwater (8 °C) was injected over a12-hr period and tracked for 13 days. A snapshot of the 3-D temperature distribution was recorded every 20 s. Figure 4 shows an example of a time profile of temperature, in response to the injection, at well C6184 (399-2-7). Water temperature dropped to around 9 °C within 1.5 hrs of the injection. The sharp increase in temperature after the initial decrease was due to a short-term malfunction in the chiller. Subsequent measurements show a mostly steady increase in temperature over time at all depths. However, at certain depths, periodic spikes in temperature of about 1 to 2 °C were evident. These intermittent temperature spikes were attributed to the operation of the sampling pumps. The wells are fitted with a single pump at a depth of around 40 ft. The operation of these pumps heats groundwater in their immediate vicinity, leading to a short temperature surge in adjacent thermistors. Pump operation also appears to cause vertical mixing within the well as evident from temperature spikes occurring at locations above and below the pump depth. Operation of the pump appears to draw cold water upward and warmer waters downward. The sensitivity of the

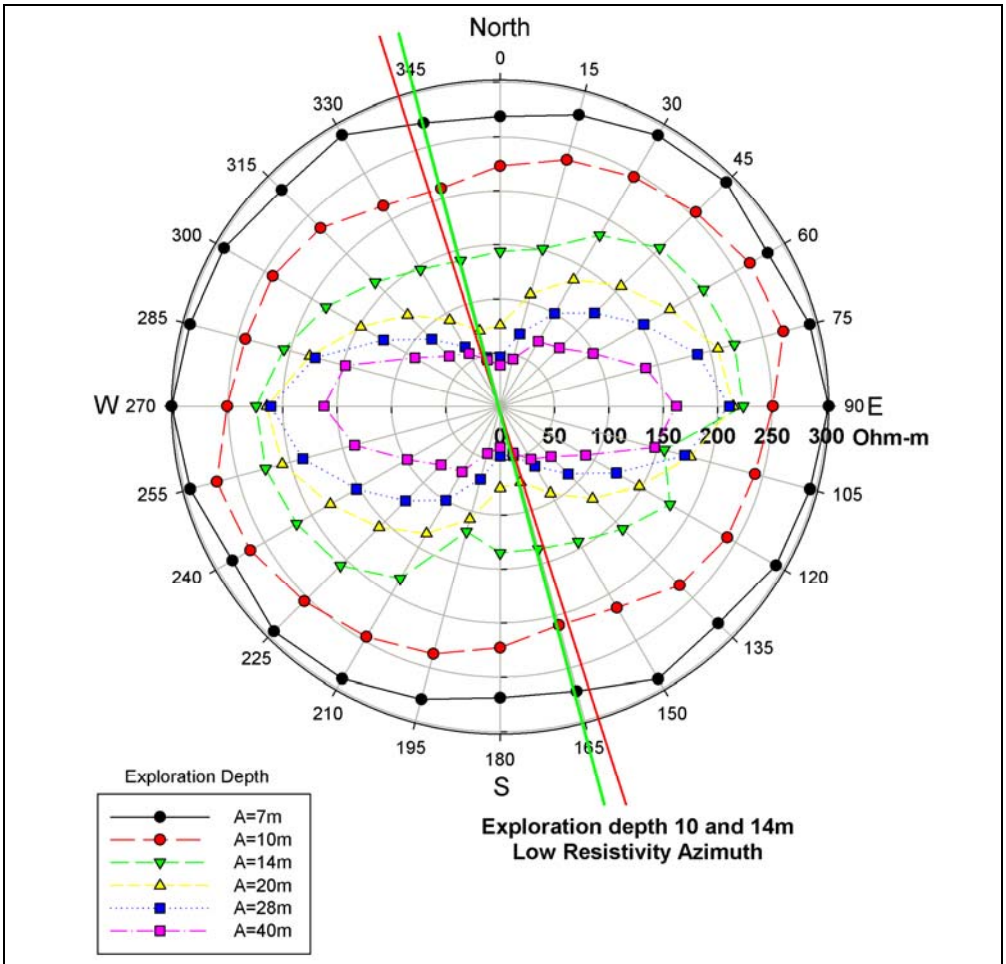

Figure 3. Square array apparent resistivity plotted again azimuth for the 7-, 10-, 14-, 20-, 28-, and 40-m A-spacings at the IFRC Well Field.

thermistor array to this phenomenon should allow quantification of vertical fluxes in the well bore, which will be critical to interpretation of tracer tests.

Temperature data resulting from this experiment are currently being processed. Based on the analyses thus far, two important observations have been made. First, the injection of chilled water showed evidence of density effects. Spatiotemporal analyses of the temperature data show the cold water essentially sinking through the formation to be transported primarily along the Hanford-Ringold interface. The combined effects of tracer concentration and the decrease in water temperature resulted in an approximate 0.002 g/cm^3 increase in density of the injected fluid that was manifest in the transport behavior of the temperature plume. Future experiments will aim for neutral buoyancy to eliminate these effects. Second, for the spatial and temporal scales examined at the IFRC site, the use of heat and bromide as tracers provide comparable information with respect to apparent transport velocities. The probability density of temperature breakthrough, computed as [T(0)-T(t)]/T(0) compared well with those derived from bromide measurements, especially in wells close to the injection point. However, as distances increase, breakthrough curves inferred from temperature show increasing evidence

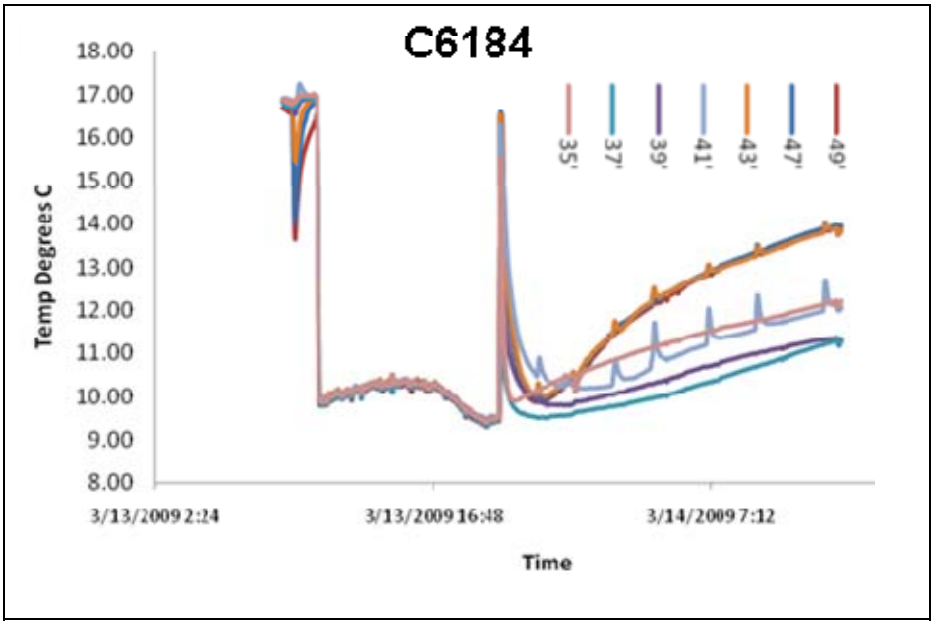

Figure 4. Temporal changes in temperature observed at well C6184 in response to the injection of chilled water.

of retardation that impact estimates of hydraulic conductivities and fluxes. Thus, differences in the transport behavior of bromide (conservative) and heat (non-conservative) should be interpreted cautiously, particularly if preferential paths are present. Monitoring heat transport at the IFRC site may provide unique insights into the magnitudes and mechanisms of groundwater movement as well as river-groundwater exchanges. A plan is being developed for a summer injection experiment that will make coupled temperature and geophysical measurements to characterize transport processes.

Geochemical Characterization

Analyses of total uranium, adsorbed U (bicarbonate extractable U), adsorption affinity (K_d) in IFRC synthetic groundwater, surface area, particle size distribution, and hydroxyl-amine extractable Fe(III) (after 30 min and 96 h) have been completed on the first 100 grab samples selected for characterization. Some of these results have been reported in previous quarterly reports, and in multiple posters presented at the ERSP Investigators Meeting in April, 2009. Correlation and geostatistical analyses of these results are underway to develop 3-D models of the U concentration inventory, and the distribution of adsorbing mineral phases and other components that control the magnitude and rate of U sorption and desorption.

One of the most important but elusive characterization measurements has been the U(VI) K_d measured in site groundwaters. As discussed in our characterization plan, these measurements are key to the development of a spatially robust surface complexation model for U(VI) adsorption for the IFRC site domain. In concept it is a simple geochemical measurement: a uranium spiked groundwater is contacted with uncontaminated sediment and the amount of adsorbed U is quantified by measuring the final aqueous concentration and taking into account the solid-water ratio. In practice,

major complications are found in determining this parameter for contaminated sediments, such as those from the SPP IFRC site domain.

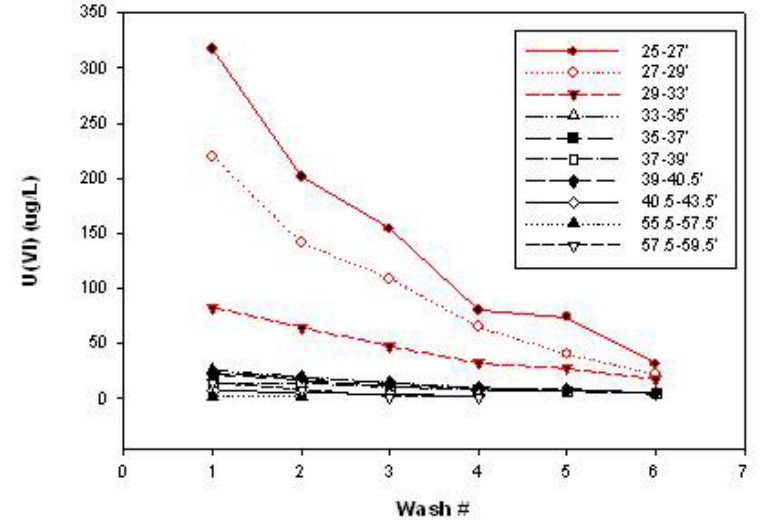

Figure 5. Desorbed U(VI) concentrations in sequential washing of Well 3-31 sediments with IFRC SGW-1.

Our first attempt to measure K_d involved the sequential washing of < 2 mm sediments ten-times with artificial site groundwater to remove the desorbable contaminant U fraction, with subsequent measurement of K_d on the washed sediments. The amount of desorbed U was quantified for each wash (e.g., Figure 5 for Well 3-31 only) providing a robust data set from which desorption K_d's were calculated. All sediments displayed a common trend, releasing greater amounts of adsorbed U(VI) in the first washes, with eventual approach to an asymptotically low value (shown for smear and saturated zone samples from Well 3-31). The solubilized U(VI) concentrations were directly proportional to the bicarbonate extractable U(VI) (BEU) in the sediment, with higher concentrations released by sediments from the smear zone. The integrated desorbed concentration for the entire sample after ten washes set averaged 0.506 +/- 0.233 of the BEU.

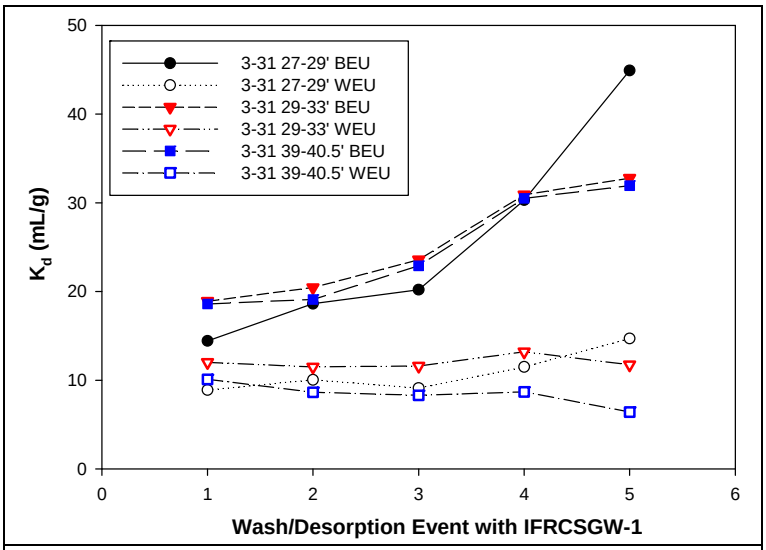

Figure 6. Desorption K_d's for select <2 mm Well 3-31 sediments calculated with bicarbonate extractable U(VI) (BEU) and water extractable U(VI) as reference sorbed states.

Desorption K_d's were calculated under the assumptions that the BEU and the water extracted U (WEU, total U extracted in 10 washings with IFRCSGW-1) represented the labile sorbed U(VI) concentration. Example K_d's for select smear and saturated zone sediments from 3-31 for the first 5 washings are shown in Figure 6. There was marked difference in the magnitude and trend in K_d, for the two reference states. Those calculated with BEU were higher, and increased

with time as the labile fraction of the BEU was depleted. Those calculated with WEU were lower and more constant, signifying that WEU was the exchangeable sorbed U(VI) fraction under the experimental conditions, and that K_d calculated with this reference state more realistically described the solid-liquid distribution process.

Surprisingly, adsorption K_d's measured on these washed (10x) < 2mm sediments using U-spiked (60 ppb) IFRCSGW-1, consistently and invariably yielded much smaller values than observed in Figure **6**; e.g., 5 times less than those calculated with WEU. These ranged between 1.5-2.1 mL/g for the sediments shown in Figure 6. In order to corroborate these lower adsorption K_d values after washing, a second set of <2mm sediments that had been extracted for 1000 h to remove labile sorbed U(VI) (BEU) were washed repeatedly to remove residual extractant HCO_3. After this cleansing, adsorption K_d was measured on these sediments using an identical procedure to that used for the sequentially washed ones. The K_d results obtained (Figure 7) showed similar values to the washed ones from Well 3-31 (e.g., those with < 20 % silt in green, ~ 2 mL/g), as well as an overall tendency for K_d increase when sediment silt content exceeded 20%.

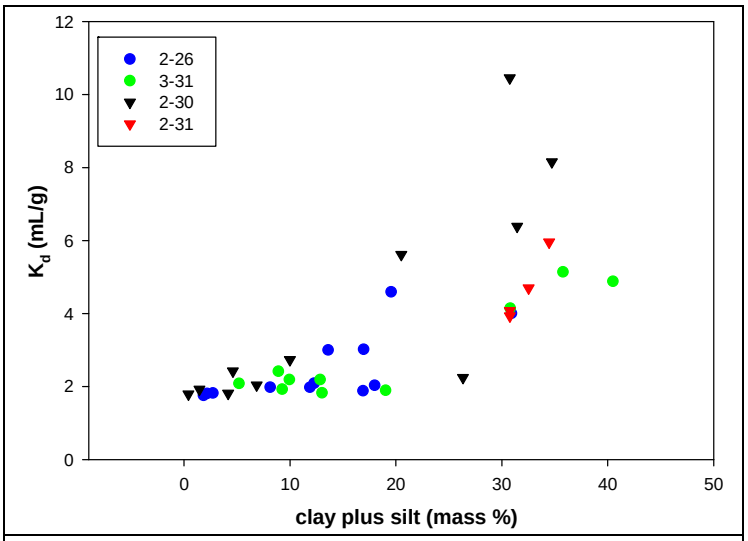

Figure 7. Adsorption K_d's measured on <2 mm sediments that had experienced 1000 h of bicarbonate extraction for removal of labile adsorbed U(VI).

Given that the sediment washing times and K_d equilibration periods were 24 h (chosen for simplicity and ease of measurement on >100 samples), we attribute the differences in the < 2mm desorption and adsorption K_d's to mass transfer, a process known to be operative in these sediments. There are details to these observations, however, that are quite puzzling, such as the apparent existence of multiple pools of labile sorbed U(VI), that provide great challenges to a characterization process that seeks measurements on a large number of samples for robust geostatistical model development.

Hydrologic Characterization

The extensive field hydrologic characterization data for the 300 Area IFRC site includes bulk formation hydraulic conductivity estimates from constant rate injection tests in 14 wells and electromagnetic borehole flow meter (EBF) test results for 26 wells. In addition, physical and hydraulic property measurements, including relative permeability-saturation-capillary pressure (k-S-p) relations, are being made on up to 40 intact core samples. The field characterization data have been used for geostatistical analyses and

for parameterization of numerical flow and transport models (STOMP and MODFLOW-MT3D) that have been used to simulate the field tracer tests.

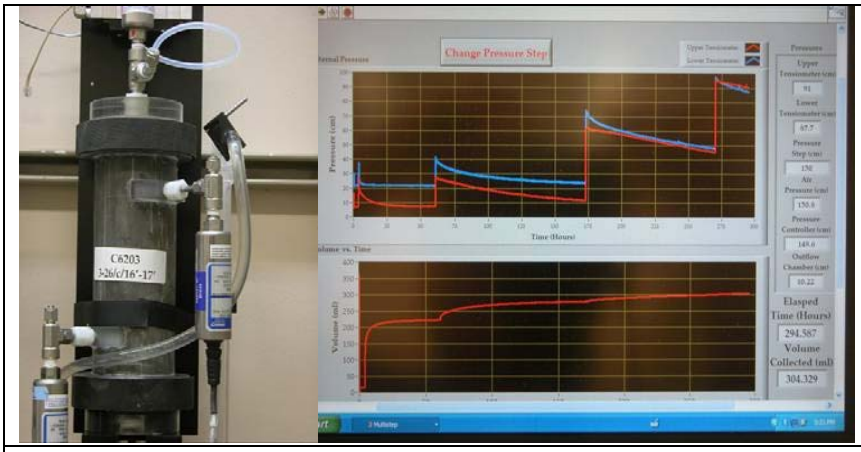

Figure 8. Intact core from Hanford 300 Area IFRC Site and data generated during a multistep outflow experiment.

The k-S-p measurements are being generated using multi-step outflow experiments. Figure 8 shows a photograph of one of the intact cores with pressure transducers attached, and the pressure and outflow data that are generated during these experiments using an automated measurement system at PNNL's Environmental Molecular Science Laboratory (EMSL). In some (~3) of these experiments, effluent data from each pressure step are being analyzed for U concentrations. We hypothesize that the smaller pore size classes will have higher concentrations of labile U associated with more reactive particles with greater specific surface area.

Geostatistical analyses have been performed on the depth-discrete field hydraulic conductivity data generated using the combined EBF and constant rate injection test data,

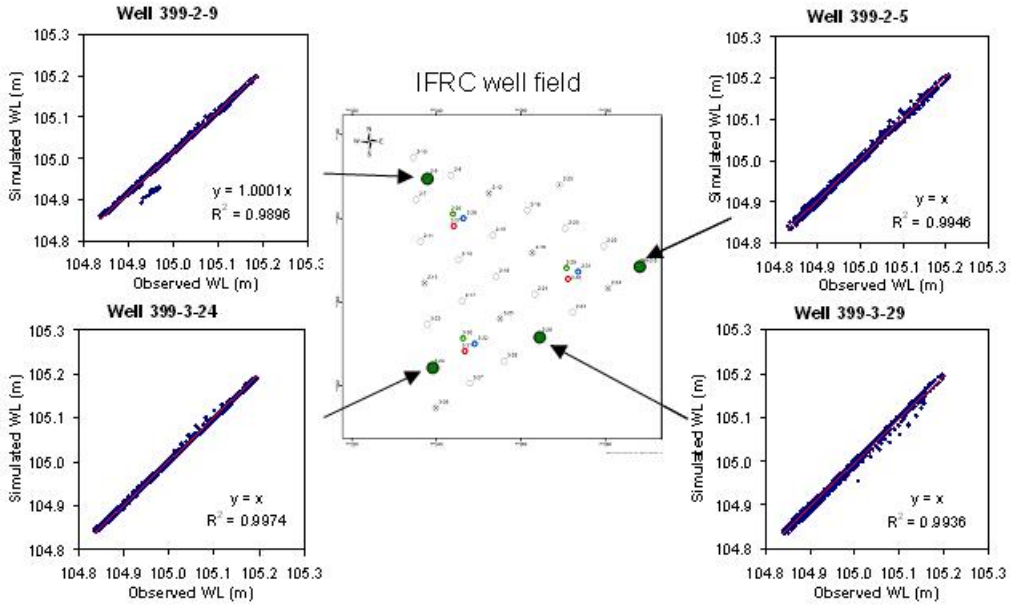

Figure 9. Comparisons of observed and simulated water level data from selected wells for the November 2008 tracer test at the Hanford 300 Area IFRC Site. Simulation results were generated using STOMP.

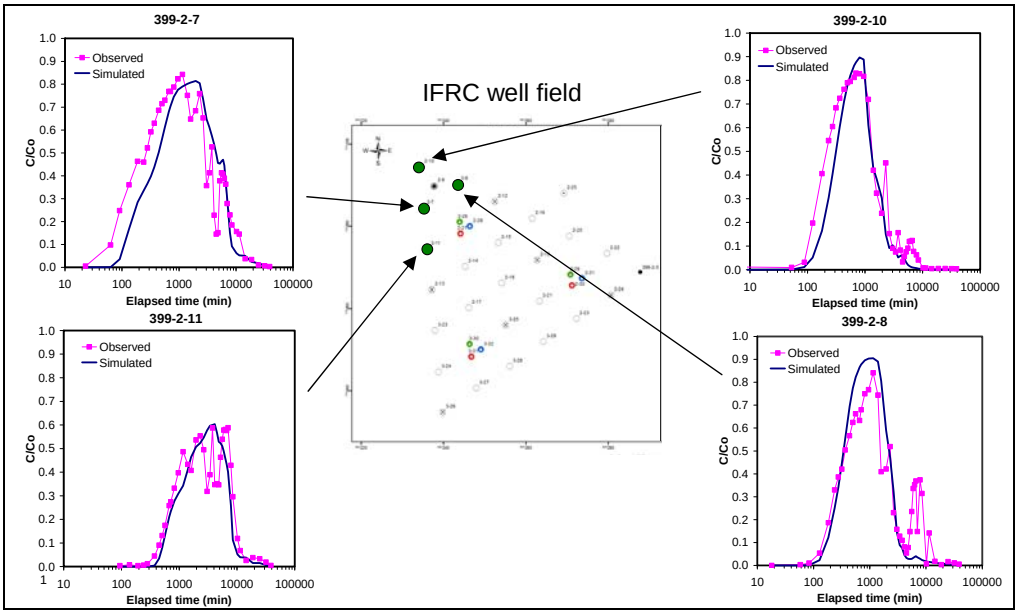

Figure 10. Comparisons of observed and simulated bromide concentration data from selected wells for the November 2008 tracer test at the Hanford 300 Area IFRC Site. Simulation results were generated using STOMP.

and on the spectral gamma log data. The latter are also being used with grain-size gamma-log correlation functions for estimating flow and transport (sorption) parameters.

Very good matches have been obtained between observed and simulated water levels for the November 2008 tracer test at the IFRC site using the STOMP simulator (Figure 9). Relatively good matches to the field bromide concentration data have also been obtained (Figure 10). Additional inverse modeling of the November 2008 experiment is being performed using the STOMP simulator coupled with parallel PEST. A manuscript describing this work is in preparation.

Task 5. Vadose Zone Experimental Program

There has been no significant change to this task since the last report. However, new characterization data is now being generated that quantifies the unsaturated water transport properties of vadose zone sediments, and contaminant U concentrations in the vadose zone and capillary fringe that will enable more accurate planning of the vadose zone experimental site and associated research opportunities. Our current plans do not call for development of the vadose zone site until FY10 and after our mid-term project review. However, our recently completed passive experiment (described below in Task 6) provides the first direct measures of U release from the smear zone and it's mixing with groundwater.

EM-40 has supported a new polyphosphate infiltration treatability study near the 300 A North Process Pond to evaluate the effectiveness of surface applied polyphosphate to

reduce U fluxes to groundwater from the lower vadose zone during periods of high water table. This two year project will develop a vadose zone infiltration site and characterize sediments from it in FY09. They will subsequently perform a polyphosphate infiltration experiment in March-April of FY10, to evaluate its effectiveness in reducing U mobilization from the smear zone. It is probable that the results of this new EM study will influence the nature of vadose zone experimentation performed at the ERSP-IFRC site.

Task 6. Saturated Zone Experimental Program

March 09 Non-Reactive Tracer Experiment

A second large-scale saturated zone tracer experiment was performed in March 2009 to assess: i.) conservative transport under a more stable hydrologic regime than was encountered during the initial tracer experiment (November, 2008), ii.) thermal transport characteristics and the efficiency of the thermistor array, and iii.) heterogeneities present in the saturated zone. Another important objective was to further refine the site conceptual model and associated numerical models. Results from this experiment, along with those from the previous tracer test, will be used to determine the experimental criteria for subsequent field-scale reactive tracer experiments.

During the March, 2009 tracer experiment, a solution containing a conservative tracer (~95 mg/L Br^- and D_2O) was cooled (~ 7 C below ambient groundwater temperature) by an industrial chiller and injected at a constant rate into well 399-2-9 (Figure 11). Tracer

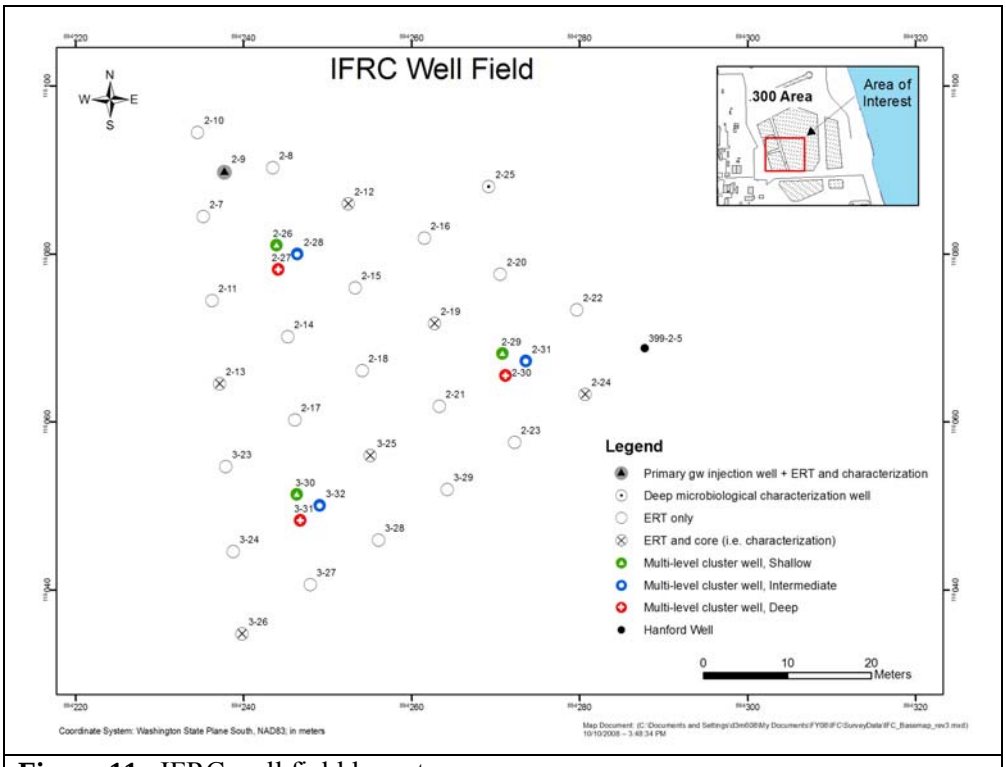

Figure 11. IFRC well field layout.

solution was injected for 567 min (~9.5 hrs) at an average rate of 71.7 gpm, for a total injection volume of ~40,600 gal. Tracer concentration and injection temperature measured in the injection well during the experiment are shown in Figure 12. The large decrease in tracer concentration and related rise in injection temperature shown near the end of the injection period resulted from a feed pump malfunction that caused the injection of approximately 1200 gal of tracer free groundwater just prior to test termination. Due to this non-ideal test termination, the chiller unit was taken off-line approximately two minutes prior to the test stop time, resulting in injection of ~140 gal of warmer water. Although the feed pump malfunction impacted observed tracer and temperature responses in the injection well, the relatively small injected volumes resulting from this occurrence did not affect the overall tracer experiment.

The injection was continued for a sufficient duration to reach ~ 40 to 80% tracer arrival at the three closest monitoring wells. The injection was then stopped, and the tracer plume was allowed to drift under natural gradient conditions. The location of the migrating tracer cloud was tracked by sampling selected monitoring wells over time and monitoring Br concentrations in-situ with downhole Ion Selective Electrodes (ISE). Aqueous samples were collected and submitted to PNNL laboratories for determination of Br^- concentration by ion chromatography. Other samples were collected for D_2O, and these analyses are ongoing at LBNL.

The observed tracer arrival in the three closest monitoring wells and a comparison with Nov. 2008 results are provided in Figures 13 and 14. Delayed arrival at the upgradient location (399-2-10) in March was due to a larger influence of natural groundwater flow on the radial flow system associated with the lower injection rate. In addition, elongation of the tracer plume in the transverse direction might also explain the earlier arrivals observed at the other two locations. Another feature of the arrival curves worth noting was the relatively dispersed arrival fronts, indicating that a range of fast and slower pathways were impacting transport processes. This response was consistent with the November, 2008 tracer test.

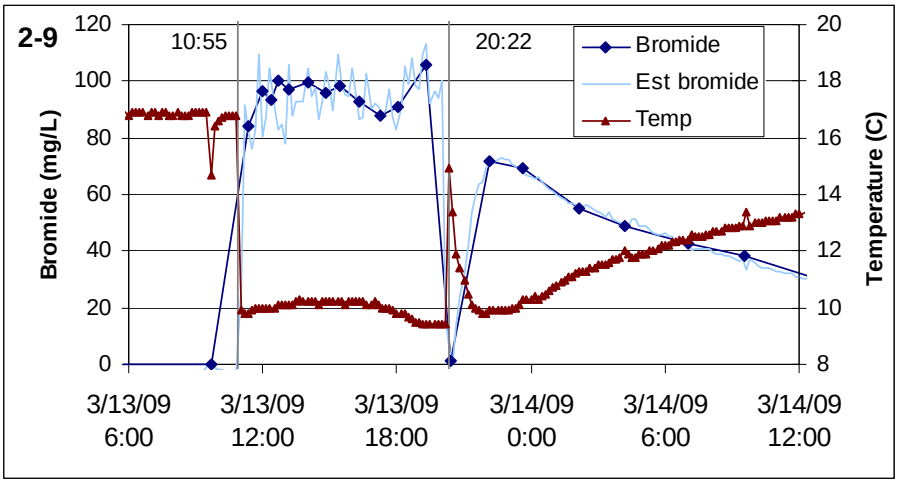

Figure 12. Tracer Concentration and Injection Concentration Measured in Injection Well 399-2-9.

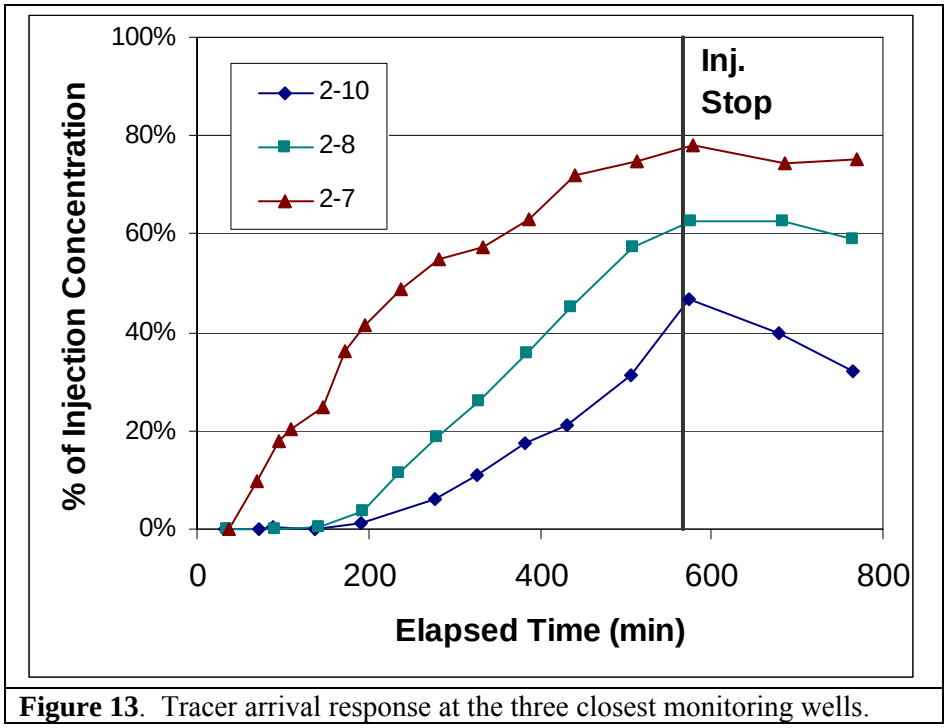

Figure 13. Tracer arrival response at the three closest monitoring wells.

Tracer concentrations were monitored for several weeks following the injection (Figure 15). 2D (plan-view) contour plots of the migrating tracer plume at different elapsed times, which represent depth/transmissivity weighted average concentrations measured in fully screened wells, were generated by creating a mixture of 2D quadrilateral and triangular elements from the well network (Figure 16). At the northernmost 3-well cluster (399-2-26, 399-2-27, and 399-2-28), an equivalent transmissivity-weighted concentration was calculated for a single centrally located equivalent well based on available depth-discrete concentration data. A number of different gridding approaches were tried, including all roughly equilateral triangular elements, isosceles triangles aligned NE-SE, and mixtures of quadrilateral and triangular elements. The contoured bromide plume results for these different gridding schemes were inspected and the best approach was selected based on overall plume shape, continuity of arrival response between well locations, and consideration of other hydrogeologic information (e.g., alignment with a potential channel feature associated with localized lows above the Hanford/Ringold contact).

The observed tracer transport response indicates the presence of a relatively narrow preferential flow path through the central portion of the well field (Figure 16). The location and orientation of this pathway is generally consistent with the channel feature discussed above and supports the hypothesis that coarser-grained, higher energy deposits of higher permeability are present within this portion of the IFRC study site.

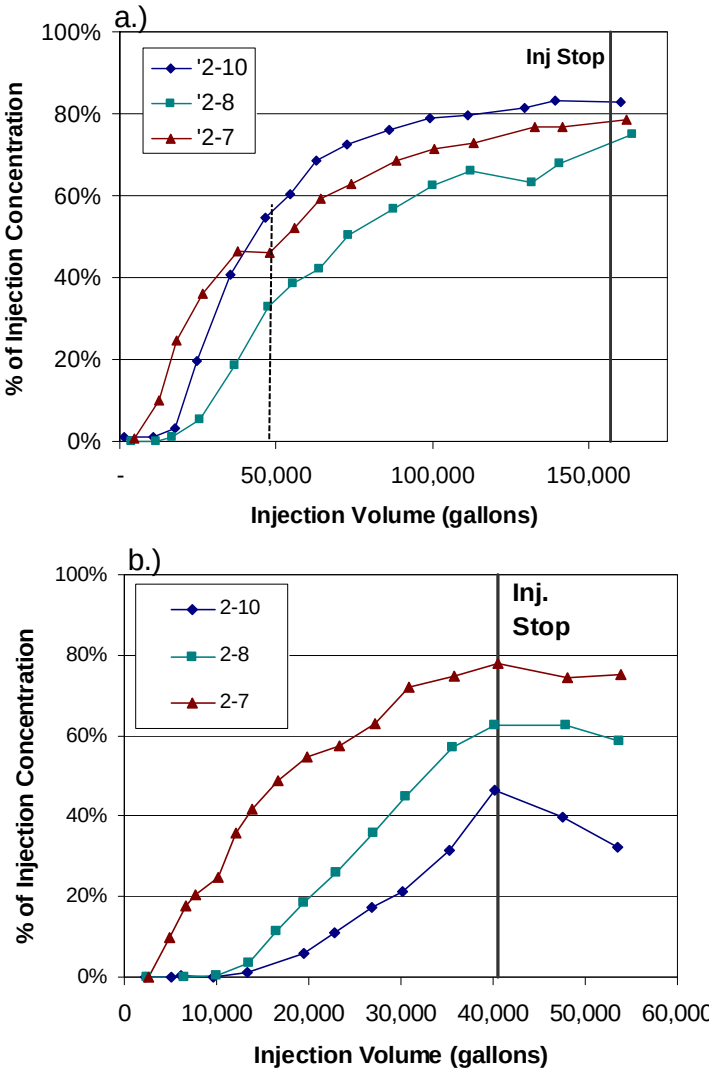

Figure 14. Comparison of a.) November, 2008 and b.) March, 2009 tracer experiment results.

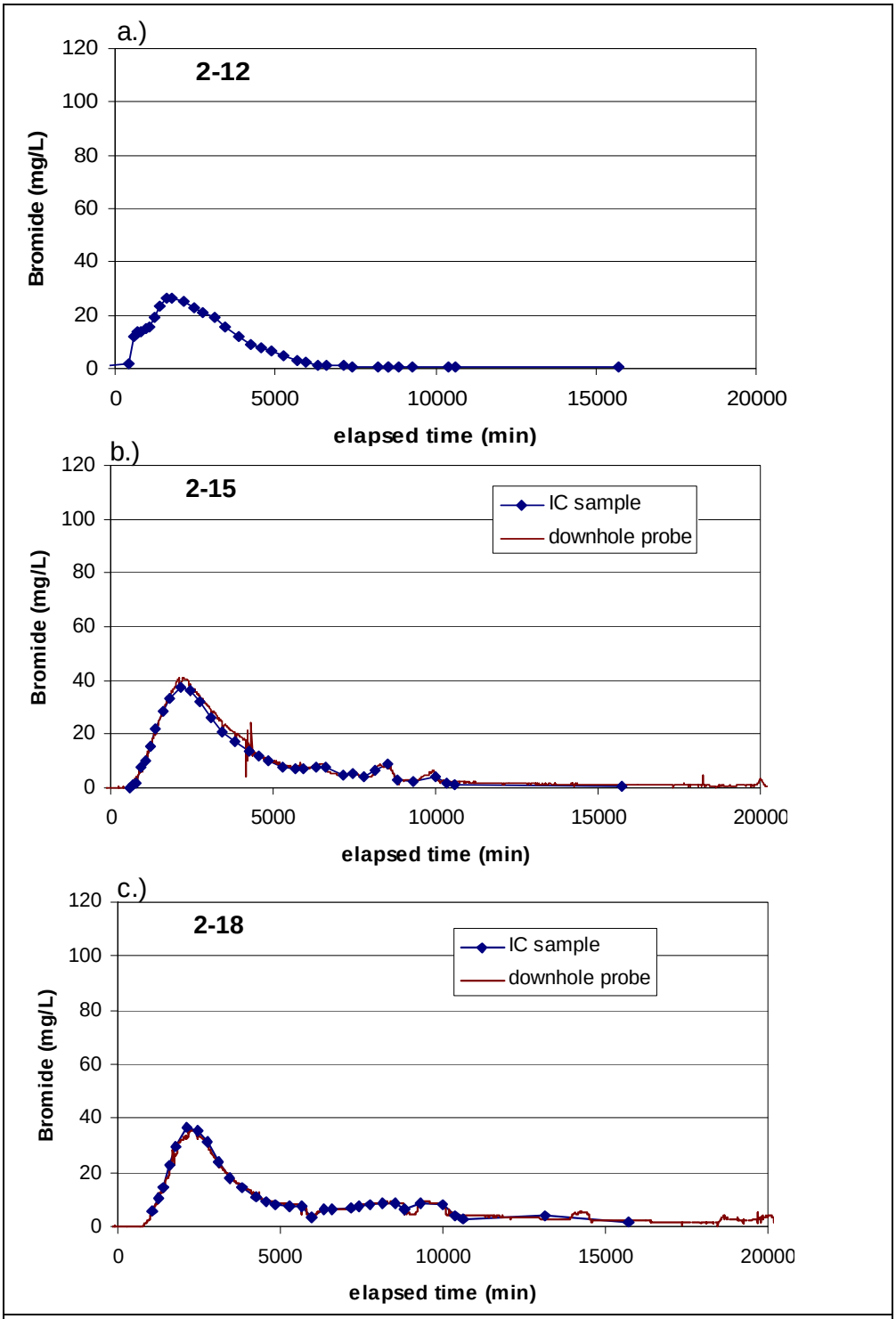

Figure 15. Tracer arrival and elution response at selected well locations.

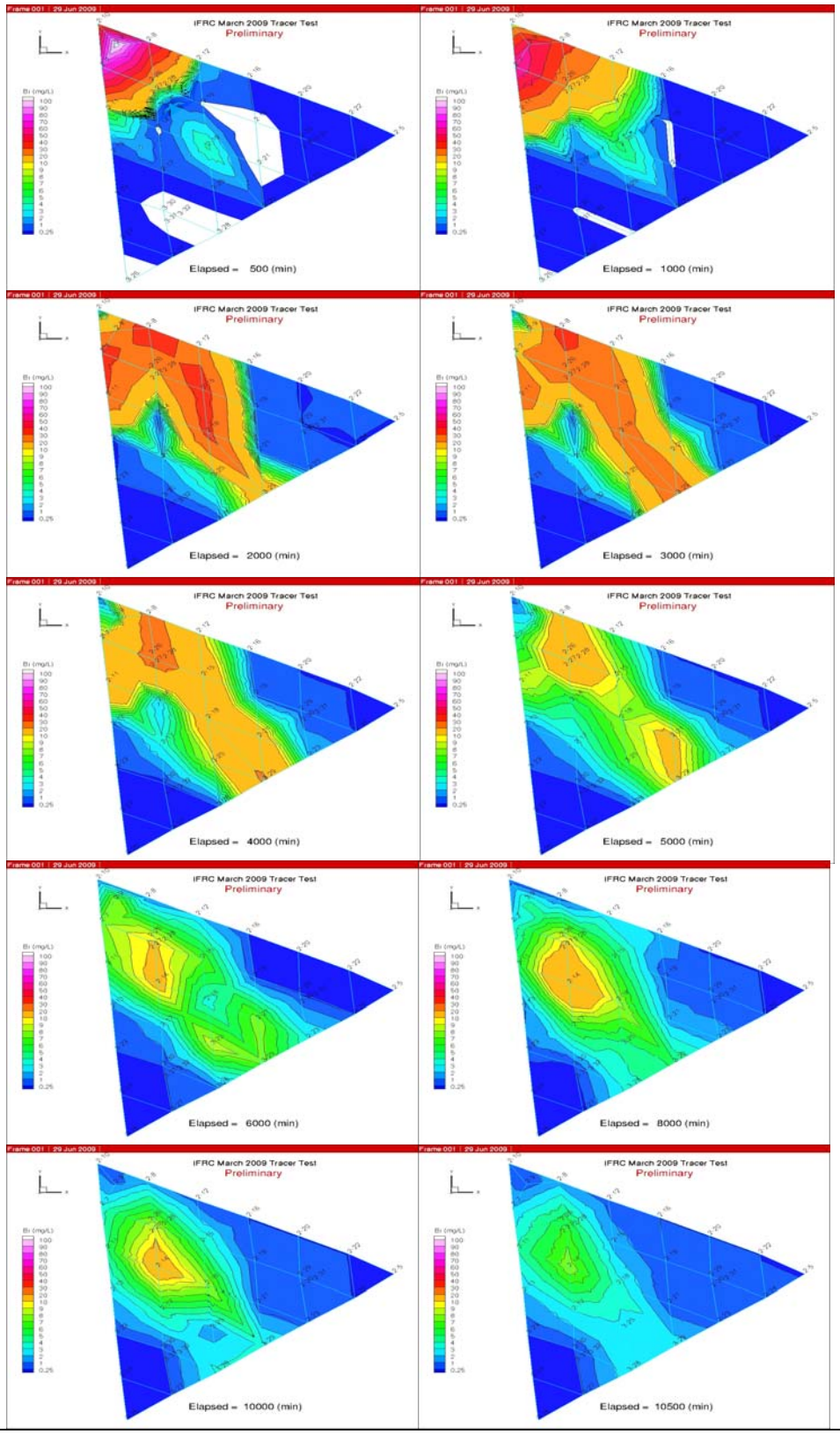

Figure 16. Contour plots of the migrating tracer plume at different elapsed times.

Also of interest is the tracer arrival and elution response at monitoring well 399-2-28. This well monitors the middle, lower permeability interval of the northernmost 3-well cluster (see Figure 11). Tracer arrival at this location is significantly delayed relative to that observed in the deep and shallow intervals, with tracer concentrations reaching their maximum value approximately 11 days into the experiment (Figure 17). Once tracer migrated into this lower permeability material, it took several weeks to diffuse back out, providing direct evidence for the influence of mass transfer on well field-scale tracer transport response.

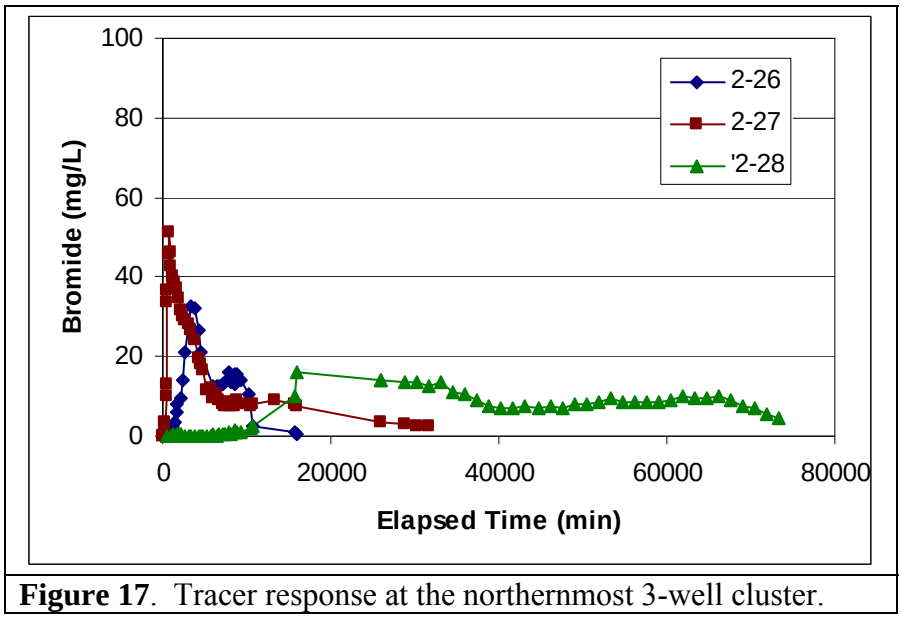

Figure 17. Tracer response at the northernmost 3-well cluster.

Spring 2009 Passive Groundwater Experiment

From the beginning of April, a passive experiment was conducted at the IFRC site to determine whether the vadose zone acts as a source of contaminant uranium to the 300 A U groundwater plume. The experiment was based on the hypothesis that uranium is released to the aquifer during the seasonal rise of the water table, and consisted of daily sampling of a subset of the IFRC wells and the specific exclusion from the site of other experiments that could perturb the natural movement of groundwater.

The experiment hypothesis was that contaminant uranium resides in the vadose zone, specifically in the 'smear zone', and is captured to the aquifer during the seasonal rise in the Columbia River during spring melt in the Columbia River headwaters. The smear zone is operationally defined as the portion of the subsurface that is above the water table at low water (generally in the fall), but below the water table at high water (generally in the spring). As the river rises, contaminant uranium is dissolved by the high water table and released into the aquifer. The U(VI) that was released to the upper most portion of the aquifer may or may not be mixed into the underlying aquifer to yield a uniform

concentration with depth. The effects of the aquifer's sweeping the smear zone may be revealed by the frequent bailing and pumping of samples from the aquifer during the spring water table rise and fall. In addition, the mixing of smear zone uranium into the aquifer can be observed by monitoring uranium and other dissolved components, particularly with respect to depth.

Except for sample collection, the aquifer was undisturbed during the test period from April 1 to July 15 (or later; the experiment is in final stages of completion). The aquifer was sampled by bailing, daily, during the test period. Thirteen wells were chosen for sampling, based on the elevation of the screen tops (the highest-topped wells were preferred), and the level of effort that was feasible (completion of sampling within a four-hour day). The bailed wells included the shallow members of the three three-well clusters (2-26, 2-29, and 3-30), and wells arrayed around the southern and eastern clusters (3-30 and 2-29) and across the well field between them. After bailing the selected set, each of the wells was sampled by pumping, using the well-field sampling system. The intermediate and deep wells of each cluster were pumped, also. To bail, a polyethylene bailer was attached to an electrical water depth tape, so that the tape would sound when the bailer was 15 cm into the aquifer. The bailer was lowered slowly to the water table and immediately removed to the surface when the tape alarmed. The water was spilled into a clean polyethylene beaker. The water was drawn into a 30 ml plastic syringe, and a 0.2 micrometer Teflon filter was attached. After rinsing the filter with 2 – 3 ml of water, 25 ml was placed in a glass scintillation vial for carbon and uranium isotopic analysis, 10 ml was placed in a pre-acidified plastic test tube for cation and uranium analysis, and 15 ml was placed in a plain plastic tube for anion analysis. An analogous set of samples was prepared from the pumped-sample system. For pumped samples, the electrical conductivity was recorded prior to sampling, using a calibrated flow cell. The tabulated conductivities were transcribed to a spreadsheet. Uranium analysis was by kinetic phosphorescence analysis (KPA); other analyses are in progress.

Selected results are shown for the 3-30 well cluster (Figure 11) in the southern quadrant of the IFRC well field that displayed some of the most dramatic

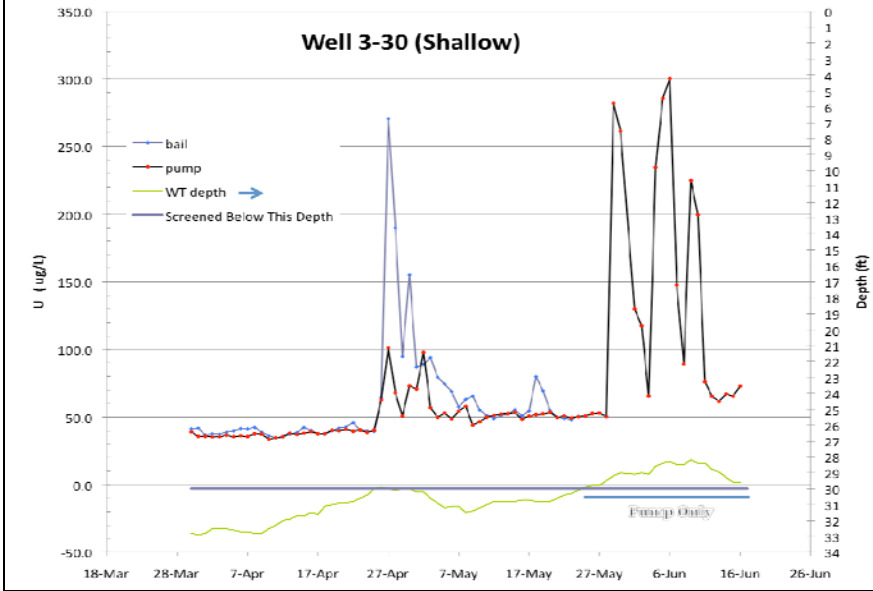

Figure 18. Uranium concentrations for well 3-30, which was completed in the uppermost portion of the aquifer. Also shown is the depth of the screen top in 3-30 and the depth to the water table during the experiment.

effects. The water table at 3-30 was at or below the screen from April 1 to May 26, allowing the top of the aquifer to be sampled by bailing (Figure 18). After May 26, the top of the water table was inaccessible. The pumped samples were produced from the middle of the screened interval, representing an approximate average of the aquifer compositon over the screened interval, but including some (unknown amount of) water drawn from above and below the screen. A comparison of bailed and pumped samples (blue and red points, respectively, Figure 18) showed a marked rise in uranium concentration during the first significant rise in the water table in late April. The concentration of uranium at the top of the aquifer increased to 275 µg/L, compared to an increase to approximately 100 µg/L in the pumped samples: the pre-rise concentration was approximately 40 µg/L. In the beginning of May, the water table fell, and the uranium concentrations dropped to approximately 50 µg/L. After May 27, the water table rose in steps to its seasonal high at a depth of 28 feet. The uranium concentration showed three sharp spikes, with a high concentraion of 300 µg/L, all in pumped samples. The aquifer-top concentration may have been higher. Although the scale of the water table depth is subdued relative to the uranium concentrations, examination of the two curves showed that each spike corresponded to a 'step' in water table depth. The aquifer, and it's dissolved U(VI) concentration, thus responded rapidly and dramatically to rises in the water table of less than one foot.

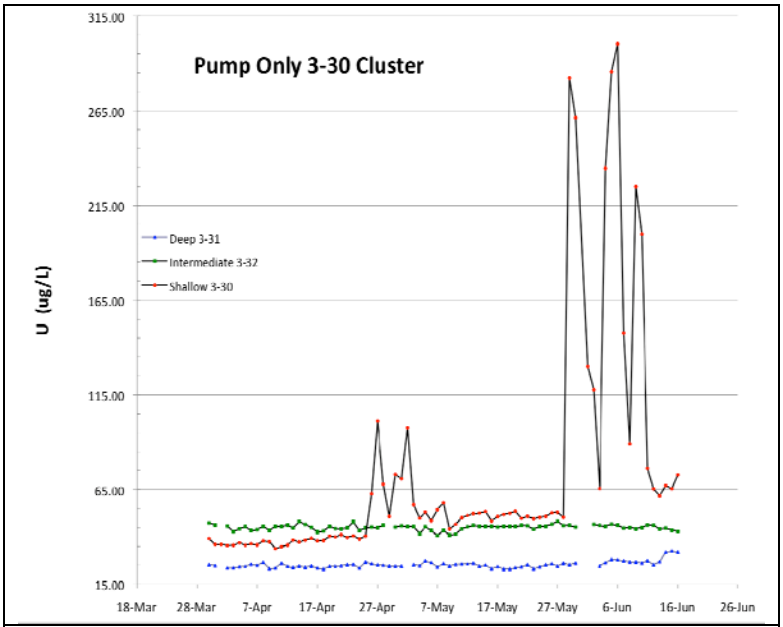

Figure 19. Uranium concentrations for pumped samples only, from all three wells in the 3-30 cluster.

Uranium solubilized from the smear zone remained localized to shallow depths of the aquifer for the duration of the experiment for which analyses have been completed (Figure 19). In March and early April, the intermediate depth samples (3-32) contained the highest concentrations of uranium, approximately 45 µg/L. After the early water table rise, the uppermost portion of the aquifer (3-30) had the highest uranium concentration. The lowermost portion of the aquifer (3-31) was always lower than the aquifer above, but its uranium concentration began to rise near the end of the reported period. (The significance of this rise is undetermined, but monitoring is ongoing.) These data indicate that the three aquifer components do not readily mix, and that the contributed uranium is isolated in the upper part of the aquifer.

Initially, the conductivity in the 3-30, 3-31, and 3-32 well cluster increases with depth (Figure 20), suggesting that the uppermost portion of the aquifer had a larger river water component, or that the deeper water was more chemically evolved (it more closely approached equilibrium with the solid phase). During the April rise in the water table, the conductivity of all samples was depressed, suggesting the introduction throughout of a river water component. During the later rise, the shallow aquifer had the highest conductivity, reaching a relatively constant value of approximately 0.46 mS/cm, but the deep aquifer conductivity rose steadily to a value of approximately 0.48 mS/cm. The central-aquifer conductivity was approximately 0.44 mS/cm at the beginning and end of the reported period. These results could be interpreted in an *ad hoc* manner, but undoubtedly represent complex interactions of site hydrology and geochemistry that will require careful analysis to understand. Their interpretation awaits further analytical results.

These preliminary results suggest that the smear zone contributes significant contaminant uranium to the aquifer during water table rise, that the aquifer does not quickly produce a homogeneous uranium concentration through its contaminated domain, and that the aquifer is not well mixed with respect to its major components. The latter two observations are surprising, considering that the rise in the water table is driven by the rise of the Columbia River, which has been hypothesized to include intrusion of river water.

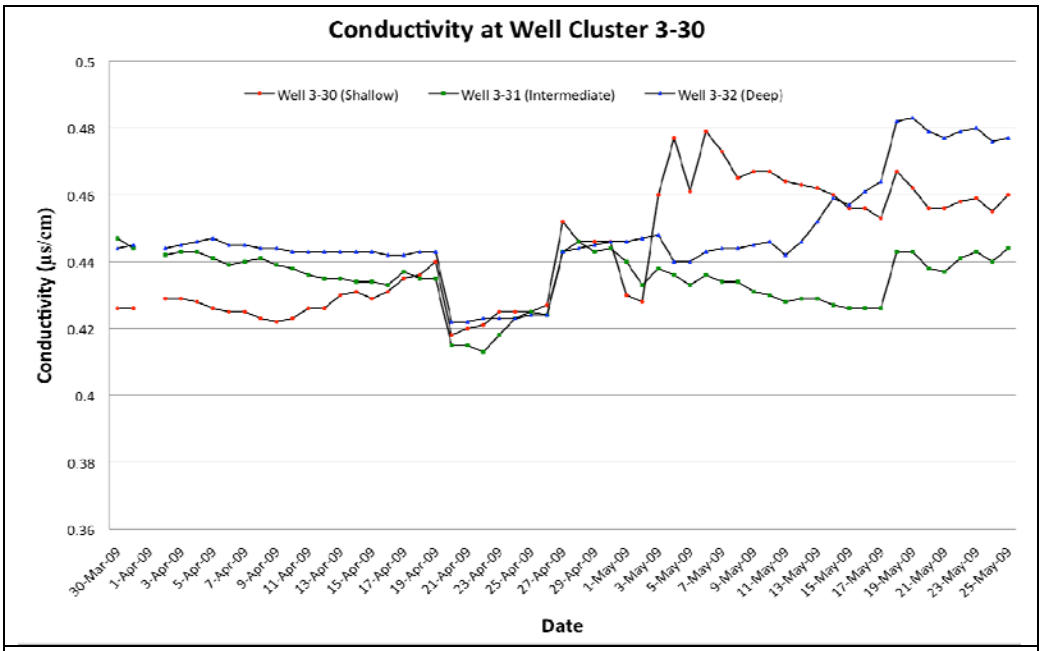

Figure 20. Pumped-sample conductivity values for the 3-30 cluster.

Additional FY 09 Field Experimental Plans

A warm month, low river stage (September-October 2009) reactive transport experiment is under planning where upgradient groundwaters of low U(VI) concentration will be

injected in the IFRC site and the plume monitored during transport to assess in-situ U(VI) desorption and mass transfer kinetics, and their linkage to previously characterized flowpath and lithologic heterogeneities. The final design for this experiment is strongly dependent on results from ongoing geochemical characterization measurements (e.g., U concentrations and forms, and spatial variation in K_d), and the intact column experiments described below.

Task 7. Modeling and Interpretational Program

Progress Summary for the Modeling Team

The modeling team has been focused on three primary activity areas over the past 6 months.

1. Establishing a robust geostatistical model for the distribution of hydraulic conductivity and related properties/parameters for the IFRC field site by integrated analysis of electromagnetic borehole flow-meter results, tracer experiment results, laboratory grain size and other analyses of borehole sediments, and down-hole geophysical measurements (MADD).
2. Developing a detailed IFRC site hydrologic model through integration of the field hydrologic and geophysical characterization results; modeling of the first (10/08) and second (3/09) non-reactive tracer experiments, including the non-isothermal experiment; and simulation of continuous temperature, electrical conductivity, and well head responses of the IFRC well field to Columbia River stage changes during the passive spring experiment (STOMP, MT3D).
3. Developing a site geochemical model (for eventual field site application) that accurately and realistically describes the kinetic adsorption/desorption process currently attributed to mass transfer by modeling U(VI) desorption and adsorption behavior measured in various large-scale and intact laboratory columns of IFRC site sediments (PFLOTRAN, STOMP). Different modeling approaches are being tried to identify the most versatile, yet realistic and robust approach for field application. The intact column study is described below.

Note that a detailed accounting of modeling team progress and accomplishments will be given in the next quarterly report (10/09).

Initial Parameterization of a Reactive Transport Model

Reactive transport experimentation with intact IFRC sediment cores (Figure 21a) was initiated in 10/08 in the EMSL Subsurface Flow and Transport Facility (SFTF) in collaboration with the PNNL SFA to begin parameterization of U(VI) multi-component reaction networks (thermodynamic, kinetic, and mass-transfer) on saturated zone IFRC sediments. Unsaturated reactive transport experiments on IFRC vadose zone sediments were initiated in 03/09 at ORNL (overseen by Dr. Scott Brooks) also as part of PNNL-SFA research. The experiments will be performed with six core sections (3 vadose zone and 3 saturated zone) using flow rates, U(VI) concentrations, and simulated

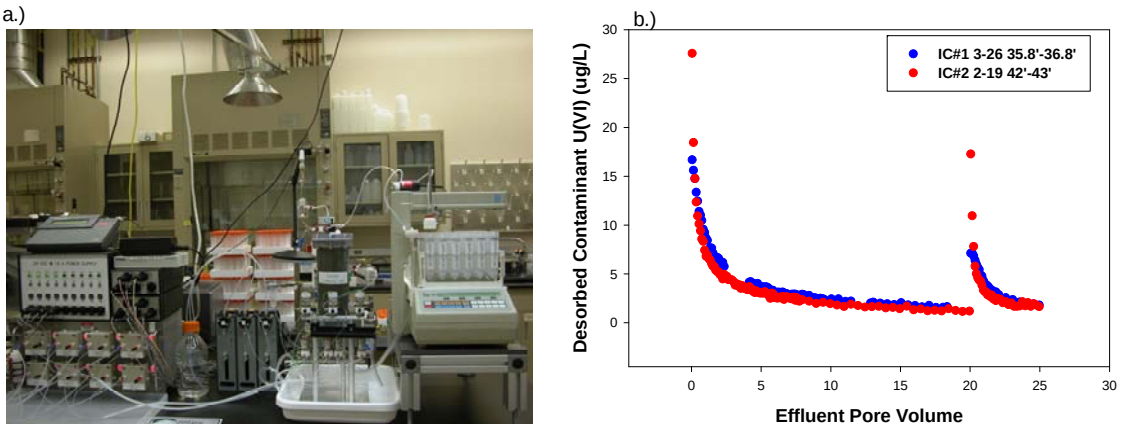

Figure 21. a.) Experimental set-up for saturated flow intact core experiments, b.) desorption of contaminant U from intact cores #1 and #2. A 48 hr stop-flow even was performed at 20 pore volume. The groundwater concentration at the time of core collection was approximately 30 ppb.

pore/groundwater compositions that closely mimic those observed at the site. This experiment series has been carefully planned by an integrated team including both experimentalists and modelers. Four different phases of experimentation (desorption of contaminant U, multi-species non-reactive tracers, adsorption/desorption of spiked U) and hydrologic characterization are being performed after which the cores will be dissected for rigorous physical and geochemical characterization. Reactive transport analyses and reaction network parameterization will be performed using both the STOMP (Rockhold) and FLOTRAN (Lichtner) codes. These results will be used for a publication on robust reaction parameter scale-up, but will also provide empirical retardation data useful in premodeling our first field reactive transport experiment with U in September-October 2009.

To date, two saturated zone column experiments have been fully completed and modeled, with another saturated zone column and an unsaturated vadose zone column in progress. The desorption behavior of contaminant U (Figure 21b) and the adsorption/desorption behavior of spiked U (Figure 22) was found to be very similar for the two saturated zone sediments studied, in spite of core origins from different aquifer depths and locations in

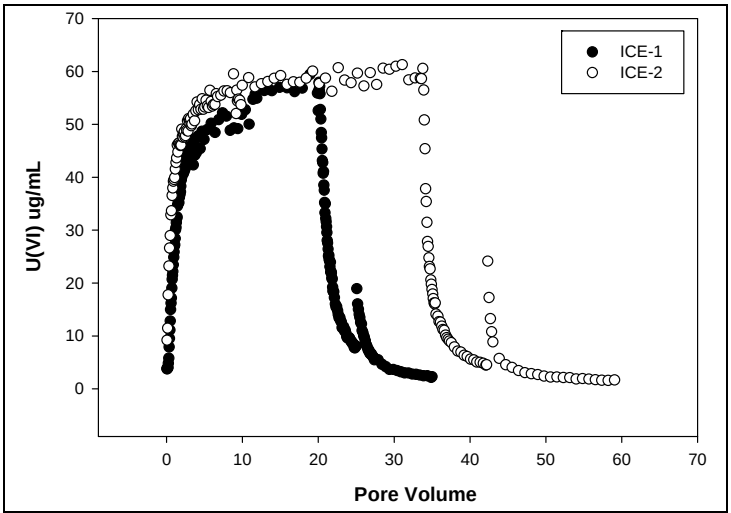

Figure 22. Breakthrough and electron behavior of a 60 ppb U(VI) pulse in synthetic IFRC groundwater. U(VI) inflow was stopped after 20 pore volumes in ICE-1 and after 35 pore volume in ICE-2. Stop-flow events occurred at 25 pore volume (ICE-) and 42 pore volume (ICE-2).

the IFRC well field. Contaminant U was released in initially high concentration, followed by slow desorption over 10 or more subsequent pore-volumes (Figure 21b). The significant spike in U concentration following stop-flow (e.g., @ 20 PV) was a clear indication of mass transfer control. The breakthrough of a pulse of U(VI)-spiked groundwater (to 60 ppb) was initially rapid (e.g., 0-4 pore-volumes; Figure 22) as a result of preferential flow-paths through the coarse-textured sediment (see, Figure 23). However, significant retardation was observed beyond that, with close to 20 pore-volumes required for full breakthrough of the influent U concentration (e.g., to 60 ppb). Uranium concentrations rebounded significantly after stop flow events in both columns during the desorption phase (e.g., @ 25 PV for ICE-1 and 42 PV for ICE-2; Figure 22) affirming the importance of mass transfer for shorter contact times.

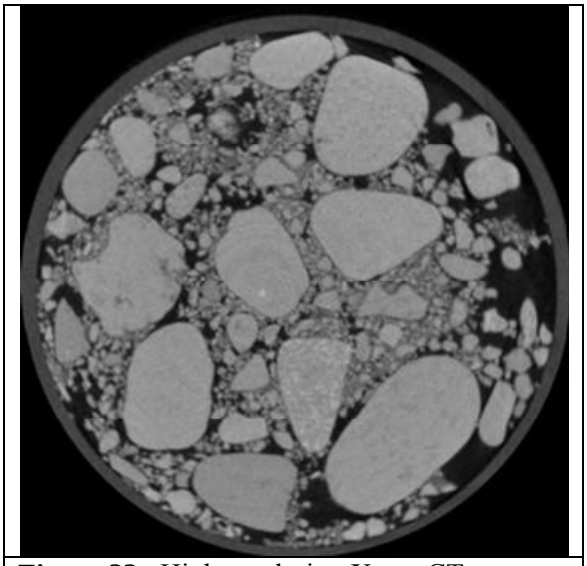

Figure 23. High resolution X-ray CT scan slice of ICE-1. One thousand slices were collected for each core for 3D reconstruction and statistical analysis.

Following completion of the reactive tracer experiments, the hydrologic properties of the cores were determined (k_{sat} and k-S-p relationships as described in Hydrologic Characterization). The cores were then shipped to the University of Texas High Resolution X-ray CT Facility for imaging of internal structure, porosity, connectivity and other physical features. Each intact core (4"x10") received 1000 scans defining "horizontal slices" of the porous media (e.g., Figure 23) that are now being assembled into 3-D images of the whole cores. The images revealed the presence of large cobbles within the cores, as well as significant "damage" along the core boundaries that resulted from the displacement of gravel during sonic core collection. These damaged areas were the probable preferential flow-paths for early breakthrough in Figure 22. Regions of intact structure, including fines-cobble interrelationships were evident in the core interiors, and were likely regions of strong U(VI) attenuation. The image slices; the 3-D reconstructions; and derived statistics on porosity, connectivity, and grain/particle characteristics will provide basis for comprehensive physical model of each core.

Our baseline dual domain, kinetic surface complexation model; developed from previous ERSP research using large repacked columns of field-textured 300 A sediments; was used as a first integration activity for the column data. These comprehensive data sets have also been provided to others in the IFRC modeling team for evaluation of different kinetic approaches. Our baseline model was well able to describe effluent U concentrations in all three experiment phases (A-desorption, B-continued desorption with non-reactive tracer addition, and C-adsorption/desorption of spike U) using a common set of adsorption/desorption and multi-rate parameters (Figure 24). Equally good fits, albeit

with a different set of equilibrium and kinetic parameters, were obtained for ICE-1 (not shown) indicating flexibility of the model to describe complex adsorption-desorption behavior in structured site materials influenced by mass transfer. The effective K_d's for the two columns that described "in-situ" adsorption-desorption behavior for the field-textured sediment were markedly different from one another (ICE-1 = 15.5 mL/g and ICE-2 = 5.6 mL/g) and higher than expected given the measured values on the <2 mm fraction of grab samples (see Geochemical Characterization). These differences will be reconciled after the cores are dissected, and the sediments subjected to size-fractionation and geochemical and physical analyses comparable to those performed on the grab samples.

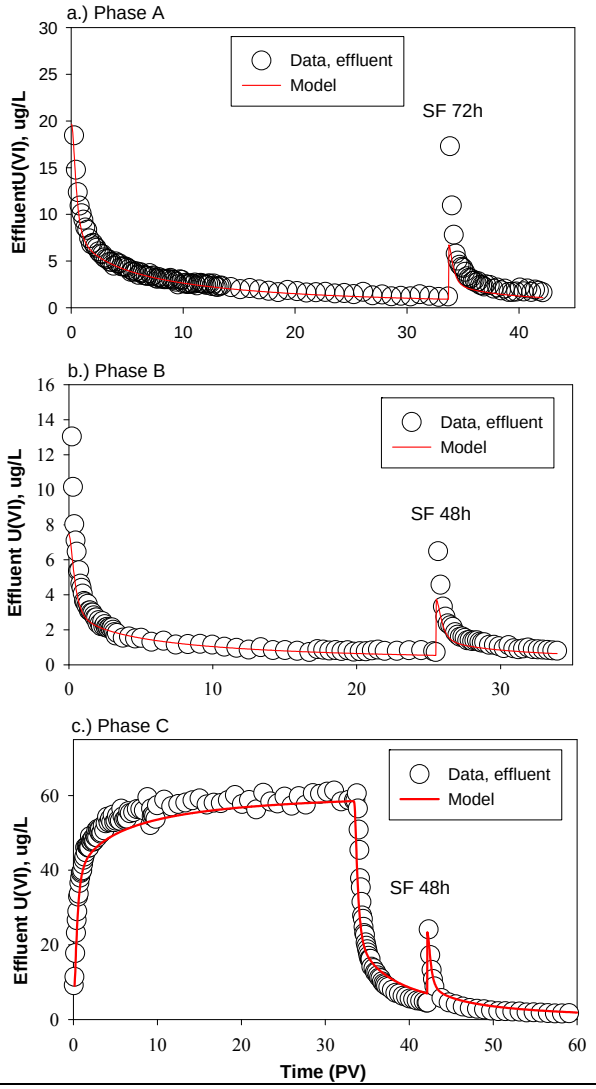

Figure 24. Modeling U(VI) concentrations in three phases of ICE-2. Phases A and B were contaminant desorption. Phase C was a spiked U(VI) pulse. A single set of multi-rate surface complexation parameters were used. Stop-flow events are noted.

Task 8. ERSD Outreach

ERSD Outreach (Site interactions, outreach, etc.)

In March, the project installed a sign at the IFRC site to orient visitors and acknowledge the support by ERSP.

Several efforts were focused on outreach and communication with regard to the IFRC to the outside community. On January 8, 2009, a presentation on the IFRC and the PNNL Science Focus Area were made to the River and Plateau Committee of the Hanford Advisory Board (HAB). A parallel presentation by Terri Stewart described activities in soil and groundwater within the DOE EM Office of Engineering and Technology (EM-20). The meeting was well attended by HAB, local DOE officials and Hanford contractors, regulators from the Environmental Protection Agency and Washington State Department of Ecology, Native American tribes, and stakeholders. A lively discussion ensued and the HAB members greatly appreciated the information about ERSP activities at the Hanford Site. A follow up to the HAB presentation was given to local DOE staff from the Richland Operations Office (RL) and the Office of River Protection (ORP) on January 28, 2009 and was similarly well received.

John Zachara and Mark Freshley, along with David Lesmes participated in a Hanford Science and Technology Workshop hosted by DOE RL and ORP on June 9-10, 2009 at Washington State University Tri Cities. The workshop was attended by over 80 people and the IFRC project was described in both the plenary session by David Lesmes and discussed in a session focused on soil and groundwater. As with the HAB meeting, the discussion of the IFRC and PNNL SFA were well received.

Mark Freshley and John Zachara, along with representatives from Lawrence Berkeley National Laboratory, Oak Ridge National Laboratory, and Savannah River National Laboratory and DOE SC Climate and Environmental Sciences Division contributed to a document "Scientific Opportunities to Reduce Risk in Groundwater and Soil Remediation." The document describes the linkages between DOE SC and DOE EM and uses the 300 Area and the IFRC as an example site to describe the interactions. The document is undergoing final clearance for publication.

V. Non-IFRC Project Activities

Limited interactions have occurred with the staff conducting the CH2M Hill Plateau Remediation Contract (CPRC) directed polyphosphate infiltration project. To date, they have completed laboratory experiments and installed a field site north of the IFRC near the North Process Pond in the 300 Area. Progress will be tracked on this project to determine further interactions.

PNNL received two replicate 1-liter samples from excavation of the 618-1 Burial Ground in the 300 Area west of the IFRC. This sampling opportunity was possible through interactions with DOE RL and completed by Washington Closure Hanford. The samples were acidic (pH = 3.7-4.2) and contain 20-60 ppm U. Other analyses will be performed on these samples as they are the first U-containing samples that we have received from Hanford that are acidic in pH, thus they provide learning opportunity. Unfortunately, the samples are in limited, but workable supply.

VI. Funding Issues

Project spending was on track with projection for the third quarter of FY 09 and there were no funding issues. At time of report writing 74.2% of FY 09 time has elapsed and 77% of funds have been spent.

VII. Upcoming Plans/Issues

The following summarize plans for the last quarter of FY09 (July-August):

- Perform small scale injection experiment during low Columbia River stage to test the ability of the down-hole ERT array to monitor real-time movement of a groundwater tracer cloud exhibiting salinity contrast.

- Complete reactive transport modeling of all three intact, saturated zone column experiments, and synthesize an initial suite of thermodynamic and kinetic parameters describing U(VI) geochemical reaction for field scale application.
- Sample and analyze monitoring wells that are nearby the IFRC during low Columbia River stage to identify a source water well for the late summer U injection experiment that preserves site isotopic integrity.
- Integrate U(VI) reactive transport parameters derived from the intact column experiments into the updated IFRC field-scale transport model.
- Premodel the planned U injection experiment over a suitable range of geochemical, hydrologic, and operational (injection rate, volume, location) conditions to optimize experimental design for hypothesis evaluation.
- Prepare injection, monitoring, and geophysical infrastructure for a large-scale U injection experiment in early FY10.
- Continue manuscript preparation, completion, and submission.

VIII. Peer Reviewed Publications, Presentations, Posters, Abstracts, and Report

Publications

De Barros, F. P. J., Y. Rubin, R. M. Maxwell. 2009. The concept of comparative information yield curves and its application to risk-based site characterization. *Water Resour. Res*., 45, W06401, doi:10.1029/2008WR007324.

Greskowiak, J., H. Prommer, C. Liu, V. E. A. Post, R. Ma, C. Zheng, and J. Zachara. 2009. Scale effects on parameter sensitivities in a dual-domain, multi-rate reactive transport system. ModelCARE 2009, International Conference, Wuhan, China. Submitted.

Harrington, S. J., B. D. Wood, and R. Haggerty. 2009. Effects of equilibrium pH and inorganic carbon on uranium transport in Hanford sediment. *Environmental Science and Technology*. Submitted.

Liu, C., S. Shi, and J. M. Zachara. 2009. Kinetics of uranium (VI) desorption from contaminated sediments: Effect of geochemical conditions and model evaluation. *Environmental Science and Technology*. Accepted.

Ma, R., C. Zheng, H. Prommer, J. Greskowiak, C. Liu, J. Zachara, and M. Rockhold. 2009. A Field-scale reactive transport model for U(VI) migration influenced by coupled multi-rate mass transfer and surface complexation reactions. *Water Resources Research*. Submitted.

Ma, R., and C. Zheng. 2009. Effects of density and viscosity in modeling heat as a groundwater tracer. *Ground Water*. Submitted.

Ma, R., C. Zheng, H. Prommer, J. Greskowiak, C. Liu, J. Zachara, M. Rockhold. 2009. Modeling field-scale uranium mass transfer at the Hanford IFRC site. ModelCARE 2009, International Conference, Wuhan, China. Submitted.

Nowak, W., F. Barros, Y. Rubin. 2009. Bayesian geostatistical design: Optimal site investigation when the geostatistical model is uncertain. *Water Resources Research*. Submitted.

Stoliker, D. L., J. A. Davis and J. M. Zachara. 2009. Characterization of metal-contaminated sediments: Distinguishing between samples with sorbed and precipitated metal ions. *Environmental Science and Technology*. Submitted.

Um, W., J. M. Zachara, C. Liu, D. Moore and K. A. Rod. 2009. Resupply mechanism to a contaminated aquifer: A laboratory study of U(VI) desorption from capillary fringe sediments. *Geochimica et Cosmochimica Acta.* Submitted.

Zang, Z. and Y. Rubin. 2009. Inverse modeling of spatial random fields using anchors. *Water Resources Research*. Submitted.

Presentations

Konopka A., X. Lin, D. W. Kennedy, and R. Knight. 2009. Hanford 300A Subsurface Microbial Ecology. Presented by Allan Konopka (Invited Speaker) at Science Focus Area Project Meeting at W.R. Wiley, Environmental Molecular Sciences Laboratory at PNNL, Richland, WA on February 26, 2009.

Konopka A., X. Lin, D. W. Kennedy, J. K. Fredrickson, M. S. Lipton, and R. Knight. 2009. Microbial Ecology in Subsurface Sediments from Hanford 300A Area. Presented by Allan Konopka (Invited Speaker) at ERSP 4th Annual PI Meeting, Lansdowne, VA on April 20, 2009.

Lichtner, P. C. 2009. Modeling Multiscale-Multiphase-Multicomponent Subsurface Reactive Flows using Advanced Computing: Application to the Hanford 300 Area. ERSP PI Meeting, Lansdowne, VA on April 20-24, 2009.

Lin X., D. W. Kennedy, J. K. Fredrickson, and A. Konopka. 2009. Distribution of microbial biomass and the potential for anaerobic respiration in Hanford Site subsurface sediments. Presented by Xueju Lin at American Society for Microbiology, Philadelphia, PA on May 19, 2009.

Mills, R. T., G. E. Hammond, P. C. Lichtner, V. Sripathi, G. K. Mahinthakumar, B. F. Smith. 2009. Modeling Subsurface Reactive Flows Using Leadership-Class Computing. SciDAC 2009, San Diego, CA.

Rockhold M., V. Vermeul, C. Murray, and J. M. Zachara. 2009. Hydrologic Characterization and Results from the First Tracer Experiment at the Hanford 300 Area IFRC Site. Pacific Northwest National Laboratory, Richland, WA.

Rubin, Y. 2009. The MAD concept and its applications in hydrogeology. Invited seminar, Chevron Research Center, San Ramon, CA. 2009.

Rubin, Y. 2009. Bayesian Geostatistical Design: Optimal Site Investigation When the Geostatistical Model is Uncertain. Presented at the European Geophysical Union General Assembly meeting, 2009.

Rubin, Y. 2009. The Method of Anchored Distributions (MAD) for Integration and inversion of IFRC hydrogeological data and for establishing a geostatistical site model, presented at the 4th ERSP Annual PI Meeting, Lansdowne, VA on April 20-23, 2009.

Rubin, Y. 2009. Inverse Modeling of Random Fields Using the Method of Anchored Distribution. Invited talk, Chevron Corp., San Ramon, CA on January 2009.

Rubin, Y. 2009. Inverse Modeling in Hydrogeology, invited lecture presented to Interagency Federal cooperation project on Multimedia Environmental Modeling. Washington, DC on June 18, 2009.

Rubin Y. A. 2009. Bayesian Geostatistical Inversion Method for Hydro Geological Data Integration in Probabilistic Risk Assessments. Waste Management Symposium in Phoenix, AZ on March 1-5, 2009.

Yin, J., R. Haggerty, J. D. Istok, D. B. Kent, and M. Rockhold2009. Experimental Investigation of the Effect of Transient Groundwater Flow on U(VI) Transport in the Hanford 300 Area. DOE ERSP Annual PI Meeting, Lansdowne, VA, on April 20-23, 2009.

Yin, J., R. Haggerty, J. D. Istok, D. B. Kent, and M. Rockhold. Experimental investigation of the effect of transient groundwater flow on U(VI) transport in the Hanford 300 Area. Isotope Hydrology and Biogeochemistry Workshop, Corvallis, OR, on June 9, 2009.

Zachara, J. M., M. D. Freshley, V. R. Vermeul, B. G. Fritz, R. D. Mackley, J. P. McKinley, M. L. Rockhold, and A. L. Ward. 2009. Hydrological Characterization at the Hanford Site 300 Area Integrated Field Challenge, Washington. Presented at the 7th Washington Hydrogeology Symposium, Tacoma, WA on April 28-30, 2009.

Zachara, J. M and the IFRC Research Team. New Results from the Hanford Integrated Field Research Challenge (IFRC). Hanford Site-Wide Seminar, Richland, WA on February 24, 2009.

Zachara, J. M., B. N. Bjornstad, J. N. Christensen, M. S. Conrad, J. K. Fredrickson, M. D. Freshley, R. Haggerty, G. E. Hammond, D. B. Kent, A. Konopka, P. C Lichtner, C. Liu, J. P. McKinley, M. L. Rockhold, Y. Rubin, V. R. Vermeul, R. J. Versteeg, A. L. Ward, and C. Zheng. 2009. New Results from the Hanford Integrated Field Research Challenge (IFRC). Presented by Allan Konopka (Invited Speaker) at DOE-ERSP 4th Annual PI Meeting, Lansdowne, VA on April 20, 2009.

Zheng, C., R. Ma, H. Prommer, J. Greskowiak, C. Liu, J. Zachara, M. Rockhold. 2009. Modeling Field-Scale Multi-Rate Surface Complexation Reactions at the Hanford IFRC Site. Presented at the ERSP PI Meeting, Lansdowne, VA on April 20-23, 2009.

Zheng, C., R. Ma, H. Prommer, J. Greskowiak, C. Liu, J. Zachara, M. Rockhold. 2009. Reactive Transport Modeling at the Hanford IFRC site. Presented at the Ground Water Summit, Phoenix, AZ.

Posters

Bjornstad B. N., J. A. Horner, V. R. Vermeul, D. C. Lanigan, and P. D. Thorne. 2009. *The IFRC Well Field: Drilling, Sampling, Well Construction, and Preliminary Hydrogeologic Interpretations.* ERSP PI Meeting, Lansdowne, VA, April 20-23, 2009.

Christensen, J. N., M. E. Conrad, J. P. McKinley, P. E. Dresel, D. J. DePaolo, and J. M. Zachara. 2009. *Uranium Isotope Systematics in the 300 Area (Hanford, WA): The Relationship Between the U Groundwater Plume and U-Contaminated Vadose Zone Sediments*. ERSP PI Meeting, Lansdowne, VA, April 20-23, 2009.

Lichtner, P. C., G. Hammond, C. Lu, R. Mills, B. Philip, B. Smith, D. Moulton, A. Valocchi. 2009. *PFLOTRAN: Application to Uranium Migration at the Hanford 300 Area*. ERSP PI Meeting, Lansdowne, VA, April 20-23, 2009.

Vermeul, V., M Rockhold, B. Fritz, R. Mackley, D. Newcomer, and J. M. Zachara. 2009. *An Initial Non-Reactive Tracer Experiment at the Hanford 300 Area IFRC Site*. ERSP PI Meeting, Lansdowne, VA, April 20-23, 2009.

Zachara, J. M. and IFC Team. 2009. *Multi-Scale Mass Transfer Processes Controlling Natural Attenuation and Engineered Remediation: An IFC Focused on Hanford's 300 Area Uranium Plume.* ERSP PI Meeting, Lansdowne, VA, April 20-23, 2009.

Abstracts

Greskowiak, J., H. Prommer, C. Liu, V. E. A. Post, R. Ma, C. Zheng, J. Zachara. 2009. Scaling effects on parameter sensitivities in a dual-domain, multi-rate reactive transport system. Abstract accepted for ModelCARE 2009.

Fredrickson J. K., J-. H, Lee, D. W. Kennedy, A. E. Plymale, A. Konopka, and J. M. Zachara. 2009. Biogeochemical redox transformations in Hanford 300A subsurface sediments. Abstract submitted to DOE-ERSP 4th Annual PI Meeting 2009, Lansdowne, VA. PNNL-SA-64801.

Konopka A., X. Lin, D. W. Kennedy, J. K. Fredrickson, and R. Knight. 2009. Microbial ecology in subsurface sediments from Hanford 300A area. Abstract submitted to ERSP 4th Annual PI Meeting, Lansdowne, VA. PNNL-SA-64871.

Kennedy, D. W., J-H. Lee, A. E. Plymale, T. Peretyazhko, D. A. Moore, J. M. Zachara, A. E. Konopka, J. K. Fredrickson **.** 2009. Microbial ecology in subsurface sediments from Hanford 300A area. Abstract submitted to ERSP 4th Annual PI Meeting, Lansdowne, VA.

Lin X, D. W. Kennedy, J. K. Fredrickson, and A. Konopka. 2009. Distribution of microbial biomass and the potential for anaerobic respiration in Hanford Site subsurface sediments. Abstract submitted to ASM 109th General Meeting, Philadelphia, PA.

Ma, R., C. Zheng, H. Prommer, J. Greskowiak, C. Liu, J. Zachara, M. Rockhold. 2009. Modeling field-scale multi-rate surface complexation reactions to quantify their impact on uranium mobility at the Hanford site. Abstract accepted for ModelCARE 2009.

McKinley, J. P., A.L. Ward, J.M. Zachara, V.R. Vermuel, C.T. Resch, J.L. Phillips, and D.A. Moore. 2009. Geochemical characterization as an experimental component in determining U transport at the Hanford Site IFRC. Abstract submitted to Migration 09

Stoliker, D. L., D. B. Kent, J. A. Davis, and J. M. Zachara. 2009. Processes controlling fate and transport of uranium(VI) in Hanford's 300-Area. Fall ACS Meeting, Washington DC, August 16-20, 2009.

Report

Bjornstad B, N., J. A. Horner, D. C. Lanigan, and P. D. Thorne. 2009. *Borehole Completion and Conceptual Hydrogeologic Model for the IFRC Well Field, 300 Area, Hanford Site* . PNNL-18340, Pacific Northwest National Laboratory, Richland, WA.